Fall 11-15-2017

EFFECT OF ALIGNMENT, SIZING, AND MANUFACTURING METHOD ON MECHANICAL PROPERTIES OF RECYCLED CARBON FIBER COMPOSITES

Nekoda van de Werken
University of New Mexico - Main Campus

Nekoda van de Werken

Candidate

Mechanical Engineering

Department

This thesis is approved, and it is acceptable in quality and form for publication:

Approved by the Thesis Committee:

Mehran Tehrani, Chairperson

Yu-Lin Shen

Mahmoud R. Taha

EFFECT OF ALIGNMENT, SIZING, AND MANUFACTURING METHOD ON MECHANICAL PROPERTIES OF RECYCLED CARBON FIBER COMPOSITES

by

NEKODA VAN DE WERKEN

B.S. MECHANICAL ENGINEERING,
UNIVERSITY OF NEW MEXICO
2014

THESIS

Submitted in Partial Fulfillment of the
Requirements for the Degree of

Master of Science
Mechanical Engineering

The University of New Mexico
Albuquerque, New Mexico

December 2017

DEDICATIONS

I would like to dedicate this thesis to my loving mother, Stephanie, and brother, Kahlil. Without their continuous support and encouragement, I would not be where I am today.

ACKNOWLEDGMENTS

First and foremost, I would like to acknowledge my advisor, Dr. Mehran Tehrani. I truly appreciate the guidance you have provided me in the pursuit of this degree. You have continuously pushed me to improve myself and to strive for excellence in my work, for which I sincerely thank you.

I would like to acknowledge my friend and colleague Pouria Khanbolouki, who provided valuable feedback and assisted with figures for this project. Additionally, Malcolm Reese contributed substantially to the two-factorial experiment for his undergraduate problems course.

I would also like to acknowledge the National Science Foundation, award #1544084, whose funding made this research possible. Last but not the least, I would like to thank Adherent Technologies Inc. for providing recycled carbon fibers and sizing.

Effect of Alignment, Sizing, and Manufacturing Method on Mechanical Properties of Recycled Carbon Fiber Polymer Composites

By:

Nekoda van de Werken

ABSTRACT

The exceptional combination of properties offered by carbon fiber composites has propelled their incorporation into high performance markets such as aerospace, wind energy, luxury cars and sporting goods. While the use of carbon fiber in these sectors is expected to continue to increase, the high price and energy cost associated with carbon fiber production acts as a significant barrier of entry into larger volume markets, such as the automotive industry. One method of navigating this transition is through the use of recycled carbon fiber composites. In addition to displacing thousands of tons of carbon fiber composite waste from landfills and incineration each year, use of recycled carbon fiber in composites has the potential to dramatically reduce the cost of composite parts while providing only slightly reduced mechanical properties.

Carbon fiber reclamation can produce fibers with up to 90% and 100% of the strength and stiffness, respectively, of virgin fibers, 25% the cost and 10-20% of the production energy of virgin fibers, and with a 99% yield. In this study, we investigate the structure and properties of recycled carbon fibers and their composites. We obtained sized recycled carbon fibers from Adherent Technologies, Inc., which are produced with a wet chemical recycling process

combined with vacuum pyrolysis. This recycling and sizing process produces carbon fibers with a low surface defect density and surface functional groups to bond with epoxies, although the reclaimed fibers form highly entangled, fluffy clumps and vary in length. Therefore, we developed an in-house apparatus to disperse and align the carbon fibers along a single axis. This technique was used to produce aligned carbon fiber mats, with up to ~0.1g cm^{-2} areal density. These mats were then infused with epoxy using a resin transfer molder (RTM) or wet-layup to produce composite plates.

Characterization was performed on the individual fibers as well as the final composite. The surface of the carbon fibers was observed with scanning electron microscopy (SEM), revealing a small amount of residual epoxy and very few surface defects. Residual particles, believed to be plastic toughener, were observed on fiber surfaces. The surface of the carbon fibers was also probed with x-ray photoelectron spectroscopy (XPS) to identify the active chemical groups of the sizing agent. The mechanical properties of the fibers were also investigated with single fiber tensile tests, which confirmed that the fibers retained ~75% of their virgin strength and 100% of virgin stiffness. The fiber alignment was characterized using image processing, which revealed that roughly 70% of fibers fell within ±15° of the mean fiber orientation. Tensile tests were performed on composite coupons, which demonstrated moderate mechanical properties. Finally, theoretical modeling of tensile strength and stiffness of composites were performed. Fiber orientation and length distributions, FOD and FLD, respectively, were taken from experimental image analysis of fiber mats and were input to the model. Effect of FOD and FLD as well as fiber-matrix shear strength were investigated. The modeling provided crucial information that can be used to guide the design of the recycled fiber composites.

Table of Contents

LIST OF FIGURES

LIST OF TABLES

Chapter 1. Introduction

1.1 Composites Overview

A composite is a material composed of two or more phases of constituents, with the goal of improving the properties or performance of each constituent. Most commonly, a composite is made up of rigid filler materials, such as a particles or fibers, which are bonded to a matrix, such as a thermoplastic or thermosetting polymer. Fiber reinforced epoxy composites are of interest for this study, as they exploit the properties of high strength, high stiffness fibers and corrosion resistant epoxy. Ideally, the matrix will protect the fiber reinforcement from environmental degradation and effectively transfer stress between the reinforcement fibers.

Carbon fiber reinforced polymer composites (CFRPs) have allowed for the development of materials with a novel combination of properties, such as low density, high strength and stiffness, corrosion resistance, long fatigue life, and controllable anisotropic mechanical properties. This combination of properties has led to the adoption of CFRPs in a diverse set of markets, such as wind energy, aerospace, infrastructure, automotive, and sports and leisure, as seen in Figure 1. However, the high price and production energy cost associated with carbon fiber composites has been a major barrier for the widespread adoption of CFRPs into large volume markets. [1]

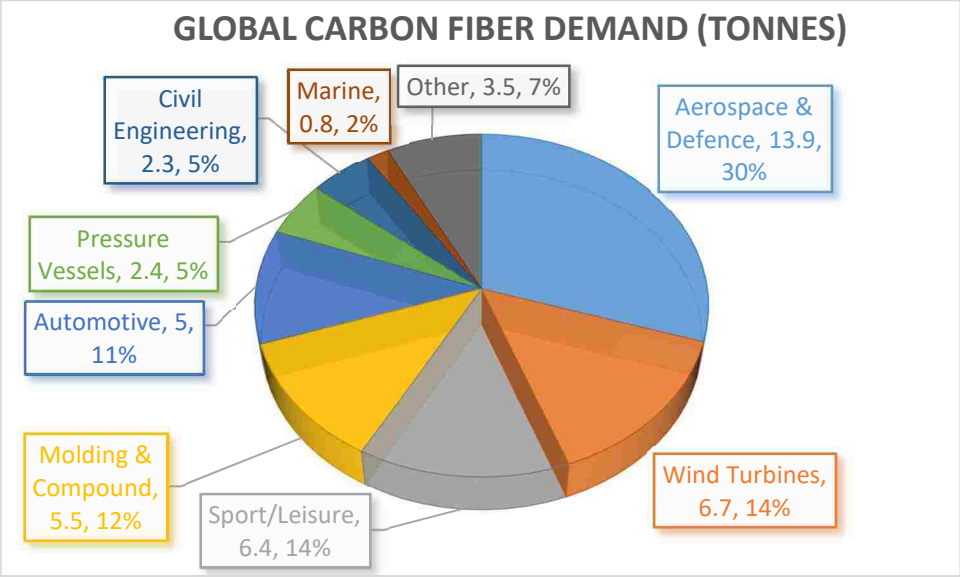

Figure 1 Global carbon fiber demand by application in thousand tonnes (2013). Total of 46.5 metric tons. [1]

Fiber reinforced polymer composites (FRP) can be categorized into continuous fiber (high aspect ratio) and discontinuous fiber (low aspect ratio) composites, as seen in Figure 2. Continuous FRPs typically have a higher fiber volume fraction, strength and stiffness, and cost compared to their discontinuous counterparts. The fibers can be aligned in a single direction, placed together in plies with various orientations, or woven together in mats corresponding to the design parameters of the application. A unidirectional composite can reach a volume fraction of nearly 65%, beyond which there is insufficient matrix to bond the fibers together. Discontinuous fiber composites are most commonly processed into randomly oriented mats, which are typically less expensive, though they also suffer a significant reduction in strength and stiffness corresponding to a drop in volume fraction and lower aspect ratio fibers. Alternatively, short fibers can also be processed into aligned composites, which can reach volume fractions near those of continuous fiber composites. [2]

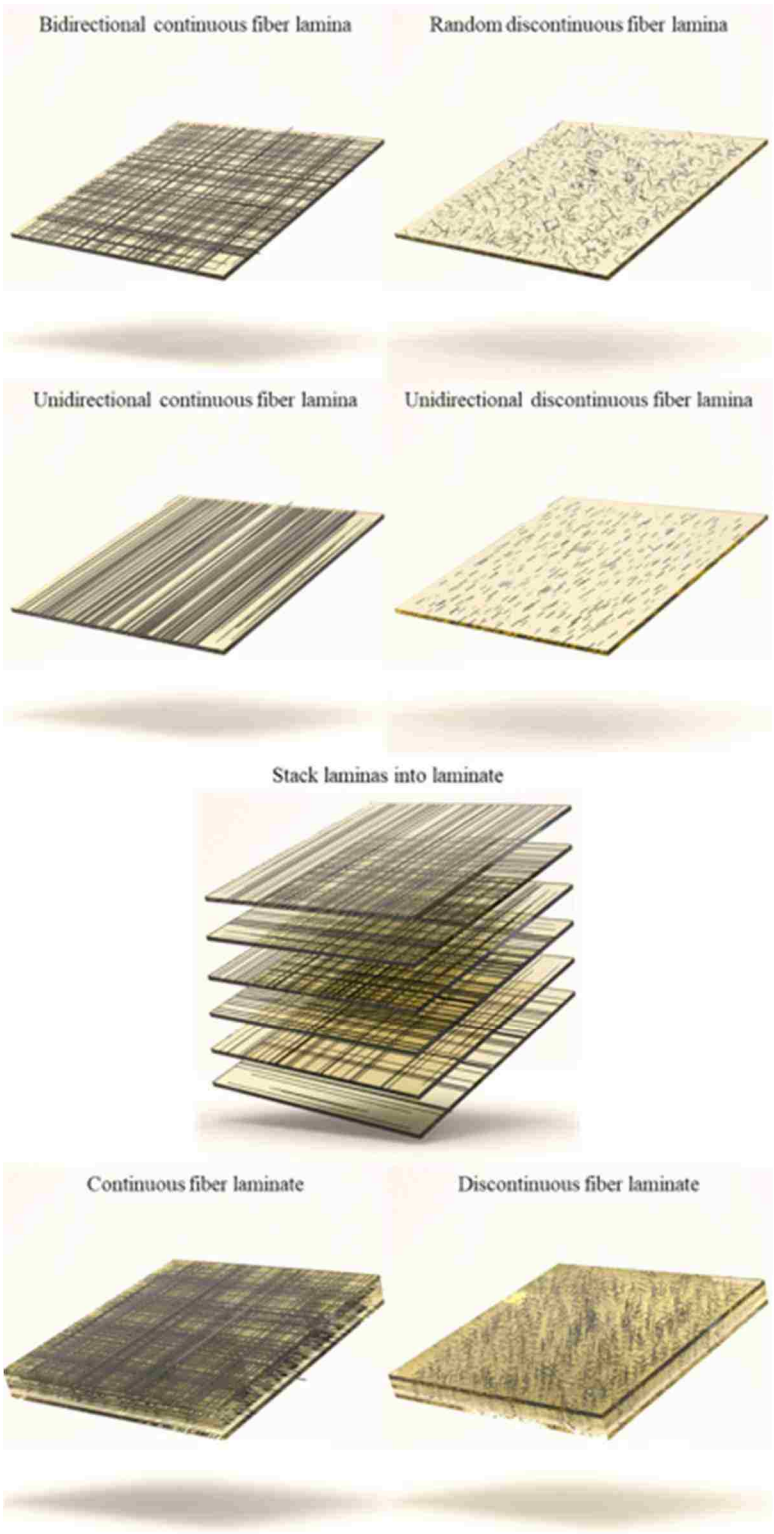

Figure 2 Types of fiber reinforce composites.

Interfacial shear strength between the fiber and matrix determines mechanical properties and failure mechanics in a composite material. A high interfacial shear strength allows for stresses to be transferred effectively between fibers and the matrix, which results in uniform stress across the cross-section of a part. Poor interfacial shear strength, however, will cause portions of the cross-section to experience higher stresses, which cannot be transferred efficiently to neighboring fibers and will result in premature part failure. A low interfacial shear strength will characteristically result in fiber pullout during failure, as opposed to fiber cleavage.

1.2 CFRP Recycling

1.2.1 Overview

The production of virgin carbon fiber is an energy intensive process, requiring 50-150 kWh/kg, which in part dictates the high price of carbon fiber composites. [3] Naturally, this high price has placed a premium on high-performance alternatives to virgin carbon fiber. One such alternative is recycled carbon fiber, which can be produced at a fraction of the cost while maintaining nearly all the mechanical properties of the virgin fibers. Carbon fiber can be reclaimed from end-of-life composites at an energy cost as low as 3-9 kWh/kg, which dramatically lowers the price compared with virgin carbon fiber [2]. Recycled carbon fiber also has the smallest effect on climate change, resources, ecosystem quality and human health when compared with landfill and incineration, the current most common disposal methods for end of life carbon fiber composites [4].

Carbon fiber composites can be recycled either mechanically or through carbon fiber reclamation techniques. Mechanical recycling involves grinding composites into small particles for use as filler in polymer matrices. Carbon fiber reclamation has been performed using pyrolysis, solvolysis, or a fluidized bed process, each with its own advantages and limitations. Mechanical recycling recovers both resin and fibers, and does not use or produce hazardous materials. However, as a filler material the mechanical properties are substantially degraded, and there are few options for re-manufacturing.

Pyrolysis recovers fiber reinforcement from a composite by burning off the polymer matrix at elevated temperatures. Pyrolysis can retain the majority of fiber mechanical properties without using chemical solvents. This process, however, can also char the surface of the fibers, is sensitive to processing parameters based on the type of composite, and emits hazardous off-gasses. The fluidized bed process is robust to many types of contamination and has been well documented, though the process can significantly degrade the fiber length and properties. This method also results in a fluffy, highly entangled fiber architecture after processing. Chemical recycling can produce fiber with very high retention of mechanical properties, though the process is not particularly robust to contamination. The recycled fibers also tend to have lower interfacial shear strength with polymeric matrices, and thus require additional sizing after recycling. [5]

1.2.2 History

Carbon fiber recycling began with mechanical recycling in late 1996, where the small ground particles were used as filler in injection molds or press molding compounds [6]. A major development in carbon fiber composite recycling was introduced in 2002 in the form of a fluidized bed process, which yielded recycled fibers with nearly 75% virgin

tensile strength, an unchanged tensile modulus, and relatively little residual epoxy on the fiber surface [7]. By 2006, carbon fiber recycling was gaining traction. The fluidized bed process had been improved, able to produce fibers with 80% virgin tensile strength, few surface defects and no measurable oxidation on the fiber surface. A catalytic recycling process was also developed at this time by Adherent Technologies Inc., which produced fibers with 83-99% virgin strength with varying degrees of oxidation. [8]

In 2008, supercritical and near-supercritical water was used to remove up to 79.3 wt% of epoxy from a composite, which was increased to 95.3 wt% with the addition of a potassium hydroxide catalyst [9]. These recycled fibers retained between 90% and 98% of the virgin fiber tensile strength. The same group also investigated the use of supercritical and subcritical alcohols for carbon fiber reclamation. This method was found to eliminate 98 wt% of resin while retaining 85-99% of the strength of virgin fibers [9]. In 2009, the use of supercritical n-propanol to reclaim carbon fibers was investigated further, which found that while the vast majority of resin was removed, the fiber surface experienced a decrease in C-OH groups [10]. This decrease is thought to be responsible for a reduction in interfacial shear strength between fibers and epoxy. Supercritical water was further investigated in recycling epoxy composites, producing clean and defect free fibers with an average tensile strength of 98.2% of virgin fibers [11].

In 2011, pyrolysis was used to recycle a carbon fiber polybenzoxazine composite in a fixed bed reactor, which produced fibers with 90% of virgin fiber mechanical properties [12]. At this point, Pimenta et. al. produced a comprehensive review and market outlook of recycled carbon fiber technology [5]. This covered a summary and analysis of various

recycling technologies, along with results of various research groups. Furthermore, various re-manufacturing techniques were compared.

Jiang et al. studied the contact angles and interfacial bonding of recycled carbon fibers, finding that T800 carbon fibers, recycled with pyrolysis, had reduced wetting and lower interfacial shear strength with thermosetting resins than virgin T800 fibers [13]. Knight et al. studied the use of supercritical water with potassium hydroxide for recycling aerospace grade epoxy composites, with positive results. They were able to remove 99.2 wt% of the resin while retaining nearly 100% of the single fiber tensile strength [14]. Li et al. used acetone and hydrogen peroxide at 60 ℃ for 30 minutes to recycle a carbon fiber epoxy composite. With this method, they were able to remove 90% of the epoxy while retaining 95% of the original strength of the fibers. Liu et al. was also able to use supercritical water and potassium hydroxide, along with phenol, to recycle a carbon fiber composite. They found little change in the tensile strength of the recovered fibers, and similar surface properties compared with the virgin fibers.

Also in 2012, Meredith et al. studied the mechanical properties of carbon fiber prepreg recycled using pyrolysis. This group compared the mechanical properties to those of the fresh prepreg and aged (out of life) prepreg [15]. They found that the tensile and flexural strength of the recycled CFRP were 65% of the fresh material, and the tensile and flexural moduli were within 90% of the fresh material. They also concluded that the recycled fibers could carry 77-82% of the peak load compared with fresh fibers. The inter-laminar shear strength of the recycled composite was 75% that of the fresh material. This same year, Morin et al. published a review of recycling processes and results, focusing on pyrolysis, fluidized bed process [7], solvolysis at low temperature and

solvolysis under supercritical conditions [16]. They conclude that solvolysis using near- or supercritical fluids is very promising, due to the relatively low environmental impact and high retention of mechanical properties and fiber length. In 2013, Xu et al. performed chemical recycling of carbon fiber epoxy composites using a mixture of hydrogen peroxide and N,N-dimethylformamide. They found that the recycling process could be carried out in 30 minutes at 90℃, removing more than 90% of the epoxy, while producing fibers with slightly decreased graphitization and more than 95% strength compared with virgin fibers.

In 2015, Sun et al. was able to use an electrochemical method to recycle CFRPs. They found that this process could produce recycled fibers with up to 80% the mechanical properties of virgin fibers. Wang et al. experimented with a recycling method using $AlCl_3/CH_3COOH$ as the degradation system for CFRPs [17]. They found that they could produce recycled fibers with a 97.43% recovery yield, while maintaining 97.77% of the virgin tensile strength, and maintaining the surface C-C and C-O bonds of the fibers. Yang et al. studied the effect of nitrogen-oxygen concentrations during pyrolysis recycling of epoxy composites [18]. They found that, under optimum conditions, only 80% of the tensile strength and modulus were preserved. Lastly, in 2016 Jiang et al. studied the structure-property relationship of recycled carbon fiber. Specifically, they examined the changes induced by the pyrolysis process [19]. They found that pyrolysis recycling results in both a decrease in fiber strength and fiber-epoxy interfacial shear strength. The fibers experience a reduction in lateral crystallite size, along with an expansion between graphitic layers. The 2-16% reduction in fiber tensile strength is thought to be related to

surface defects introduced in the process, while the 24% reduction in IFSS is related to a 2.6-42% decrease in surface oxygen concentration.

1.3 rCFRP Remanufacturing

Various re-manufacturing methods have also been developed for recycled carbon fiber composites. Many methods that have been developed for discontinuous fiber composites can also be applied to rCFRPs, and are worth reviewing as well. These processes typically produce uniform aligned or randomly oriented composites. Randomly aligned composites typically reduce the cost of remanufacturing, but observe a corresponding reduction in volume fraction and thus composite properties. An overview of aligned short fiber composites was provided by Such et al. in 2014 [20], beginning with the first instances of fiber alignment methods developed in the early 1960's.

In 2008, a polyethylene recycled carbon fiber composite with 30 wt%, with randomly oriented fibers, was produced in 2008 [21]. This composite was measured to have a strength and stiffness of 22.3 MPa and 724 MPa, respectively. In 2010, Turner et al. outlined a portion of the challenges in improving the performance of recycled carbon fiber composites, concluding that fiber alignment would be a critical factor in producing competitive recycled fiber composites [22]. They were able to produce a recycled carbon fiber composite with 44% volume fraction, with a strength and modulus of 422 MPa and 80 GPa, respectively, using compression molding with 5-10 MPa molding pressure.

In 2010, Wong et al. used a solution of hydroxyethyl cellulose, surfactant, and anti-foaming agent with an axial impeller to disperse the fluffy clumps of recycled fibers [23]. The fibers were further processing in a baffled tank with a radial impeller to increase

shear forces. This same year the incorporation of multiple carbon fiber phases, particularly individual fibers and fiber bundles, was examined and found to considerably toughen the composite through complex failure mechanisms [24]. Turner et al. also studied the effects of parameters of the recycling process on average length of the recycled fibers [25].

In 2012, Pinho et al. studied the compressive failure of unidirectional and woven recycled and virgin CFRPs, also concluding that multi-scale fiber bundles in recycled CFRPs contributes to complex failure mechanisms [26]. Wong et al. worked to increase the interfacial adhesion between recycled carbon fibers and a polypropylene (PP) matrix [27]. They found that the addition of a coupling agent could increase the tensile strength by 150%, from around 50 MPa to 125 MPa. They attribute this increase partly to the increase in interfacial shear strength from 2.36 MPa to 7 MPa.

The mechanical properties and morphology of recycled carbon fiber reinforced nylon 6 composites was studied by Feng et al. in 2013 [28]. In this study, the group modified the surface of the recycled carbon fiber with nitric acid and an epoxy macromolecular coupling agent. They found a significant increase in interfacial adhesion, along with an increase in the mechanical properties. Specifically, for a 20% volume fraction composite, the tensile strength increased form 120 MPa to 170 MPa and the modulus increased from 13 to 19 GPa. Stoeffler et al. was able to produce a polyphenylene sulfide (PPS) reinforced recycled carbon fiber composite with up to 40% volume fraction. The composite used short fibers and was measured to have a tensile strength and modulus as high as 200 MPa and 30.3 GPa.

In 2014, Okajima et al. found that supercritical methanol could be used to recycled CFRPs without disturbing the shape of the plain fabric while reducing the tensile strength of the fibers by less than 9% [29]. Pimenta et al. studied the influence of micromechanical properties and reinforcement architecture on the mechanical response of a recycled composite [30]. It was found that fiber bundles can increase the toughness of a composite by an order of magnitude without significantly reducing the composite strength or stiffness. Also in 2014, Yu et al. developed the High Performance-Discontinuous Fibre (HiPerDiF) method [31]. This method was used to successfully align 67% of 3 mm long tape type preforms within the range of ± 3 degrees. The composite made from these aligned fibers had a volume fraction of 55%, with a strength and stiffness of 1509 GPa and 115 GPa, respectively. While this technique may be applicable to recycled carbon fiber, the alignment of recycled carbon fibers was not covered in this study.

1.4 Summary of Present Work

The aim of this investigation was to determine the effect of alignment, sizing, and manufacturing method on the properties of recycled carbon fiber epoxy composites. Recycled carbon fibers were obtained from Adherent Technologies Inc., a carbon fiber recycling company based in Albuquerque, NM, USA. The fibers were recycled using a catalyst-based wet recycling process with a vacuum pyrolysis treatment. A polymer sizing is then applied to the recycled fibers, tailored to maximize the interfacial adhesion to the epoxy system chosen for this study. The recycling process produces fluffy, highly entangled clumps of fibers as seen in Figure 3.

Figure 3 As received recycled carbon fibers from Adherent Technologies, Inc.

The surface of these fibers was characterized with scanning electron microscopy (SEM) and x-ray photoelectron spectroscopy (XPS). SEM was used to observe any residual epoxy or surface defects, such as pitting, on the fiber surface. XPS was used to identify chemical groups on the surface of the carbon fibers to ensure that the sizing can be expected to form strong bonds with the epoxy. This adhesion to the polymeric matrix was also investigated using single fiber fragmentation tests to characterize interfacial shear strength. The tensile strength and modulus was also measured directly with single fiber tensile tests.

A centrifugal alignment method was used to produce aligned recycled carbon fiber (rCF) mats for composite manufacturing, similar to that developed by Pickering et al. at the University of Nottingham [3] as seen in Figure 1. The recycled fibers were processed and stacked into 1mm, highly aligned mats. The fibers were dispersed in a viscous glycerol solution with an axial impeller. Once fully dispersed, the fiber slurry

was run through a convergent nozzle and deposited on a nylon mesh inside of a rotating drum. The rotation of the drum created sufficient centrifugal force to expel the glycerol solution through the mesh, while the fibers were deposited on the mesh. This glycerol was collected with a cylindrical containment surrounding the rotating drum, fed into a 1-liter beaker and recirculated with a pump. The difference in velocities of fiber slurry and the rotating drum forces the fibers to align along the circumference of the drum. The nozzle reciprocated along the axis of the drum, depositing fibers continuously along its motion to create the width of the mat.

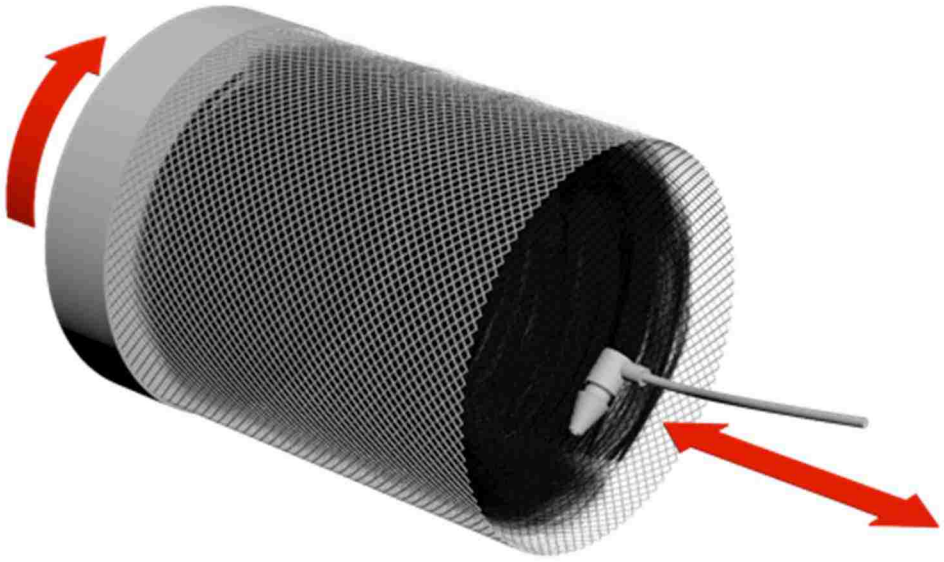

Figure 4 Centrifugal alignment rig schematic. Glycerol containment not shown for clarity.

A two-factorial experiment was used to optimize the processing conditions of the alignment rig. The parameters of interest were drum rotational speed, total mat thickness, linear reciprocal velocity, and solution viscosity. The alignment was characterized using light microscopy and image analysis software. Once the optimal parameters were found,

ten thin aligned mats were processed for each composite plate to achieve a desired thickness of 1 mm.

The non-aligned rCF composites were processed using a vacuum filtration method. The fibers were dispersed in a viscous glycerol medium before being poured onto a sieve attached to a vacuum Erlenmeyer flask. This process was repeated until a sufficient mass of fibers was deposited onto the mat. A vacuum was pulled after each new batch of fibers was added to remove any excess glycerol and compact the fibers in the mat. The mats were thoroughly rinsed with warm water and dried before being infused with epoxy.

The tensile strength and modulus for the aligned and non-aligned composites were measured. The fractured surfaces were analyzed with SEM to identify failure mechanisms. Cross-sectional microscopy was performed to determine volume fraction, fiber alignment, and void content.

The mechanical properties of composites were correlated to the composite manufacturing method (i.e., hand lay-up and resin transfer molding), fiber sizing, and to the degree of alignment within each composite. As expected, sizing and alignment were found to improve the strength and elastic modulus of the composites. Resin transfer molding was also found to produce superior properties compared with wet layup. This was due to a high void content in wet-layup parts, which was not present in RTM composites.

Lastly, a model was used to approximate the fiber length and orientation distributions that were experimentally determined. The mechanical properties of the

composite were calculated using these distributions, along with estimated critical length values. The relationship between fiber length, orientation, and critical length with composite strength and stiffness was then investigated.

Chapter 2. Single Fiber Characterization

2.1 Recycling Process

Recycled carbon fibers were acquired from Adherent Technologies Inc. (ATI), a company based in Albuquerque, NM, that has been in the composites recycling industry for over two decades. ATI uses a combination of a catalyst-based wet recycling process with a vacuum pyrolysis treatment to produce the recycled carbon fibers [32]. ATI claims that this process can successfully reclaim 99.5% of carbon fibers from a composite, with a reduction in strength of less than 10%. However, this process leaves the surface of the fibers unreactive, which is not suitable for re-manufacturing into a high-performance composite. Therefore, ATI also added a sizing polymer to the surface of the recycled carbon fiber, which is designed to enhance load transfer between fiber and polymeric matrix. Both sized and non-sized fibers were collected for comparison in this study, which require additional processing to produce highly-aligned and densely packed mats suitable for re-manufacturing.

2.2 Sizing Process

ATI has formulated different carbon fiber sizing agents for a selection of polymer matrices. The sizing procedure utilized an aqueous based emulsion consisting of a reactive coupling agent, a film-forming polymer carrier, a surfactant, and a solvent. The fibers were dipped into the emulsion to achieve a 200-500 nm thick surface coating. The fibers were then air dried and subsequently heat treated to activate the coupling agent. Finally, the fibers were rinsed with acetone to remove any excess material. The coupling agents in the emulsion form bonds with the basal plane crystallites of the carbon fiber,

along with edge and defect sites. The adhesion promoting coating has been shown to improve the mechanical properties of virgin carbon fiber composites, and was used here to further investigate its effect on recycled fiber composites. [33]

2.3 Surface Characterization

The mechanical properties of carbon fiber are particularly sensitive to the microstructural characteristics and surface defects [34]. Specifically, flaw size and density on the fiber surface have a significant effect on the tensile strength of the fiber. Additionally, residual polymer or particle contaminants may reduce the performance of remanufactured composites, and are therefore of interest. Scanning electron microscopy (SEM) was utilized to observe the fiber surface and characterize the prevalence and severity of such defects.

The fiber surface was also characterized with x-ray photoelectron spectroscopy (XPS). This technique can be used to identify the quantity and type of elements and chemical bonds present on the surface of a material. In general, these functional groups can be correlated to the interfacial shear strength of epoxy-fiber composites, as they are expected to form strong bonds with the polymer matrix.

Lastly, the interfacial shear strength was investigated with single fiber fragmentation tests. These tests can be used to determine the critical length of a fiber/epoxy system, which can then be used to calculate the interfacial shear strength. These tests were performed on virgin carbon fiber, as-received sized and non-sized fibers, and on processed fibers. Unfortunately, the results obtained in this study were inconsistent, explanations for which are explored in detail in Section 2.3.3.

2.3.1 Scanning Electron Microscopy

The size and non-sized carbon fibers were imaged using SEM. A FEI Quanta 3D FEG SEM was used for this imaging. The images were used to analyze the potential defects, such as pitting, residual epoxy, or foreign contaminants that may have been introduced during the recycling or sizing processes. Additionally, these images were used to measure the carbon fiber diameters. The fibers were attached to the sample holder using conductive carbon tape. Representative SEM images can be seen in Figure 5.

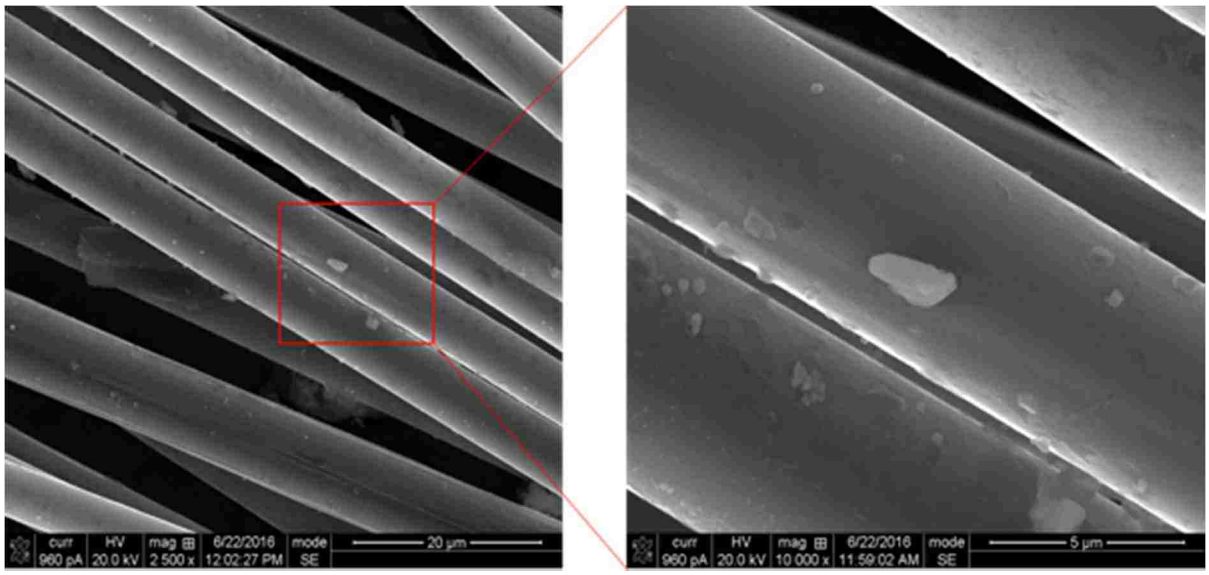

Figure 5. SEM images of the non-sized recycled carbon T800 fibers at 2,500x (left) and 10,000x magnification.

These images show the presence of some residual polymer, likely toughening particles added to the epoxy, appearing as lighter contrast spheres on the fiber surface. A small amount of residual epoxy can also be observed on several fibers as darker domains on the surface. Slight pitting was also observed on the fiber surface, which tends to result

in decreased fiber strength. These images were processed with the image analysis software ImageJ to determine the fiber diameter, which was measured to be an average of 5.5 µm, which is slightly larger than virgin T800 fibers. An example of the diameter measurement is shown in Figure 6.

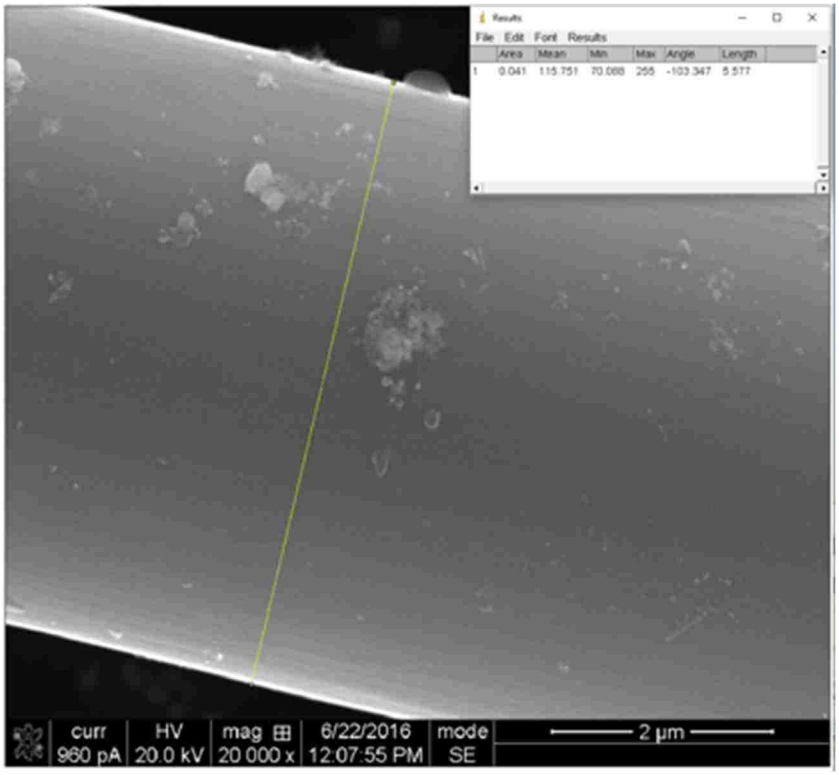

Figure 6. Diameter measurement of non-sized recycled carbon fiber using ImageJ (20,000x magnification).

2.3.2 X-ray Photoelectron Spectroscopy

The recycled carbon fiber surface was also characterized with x-ray photoelectron spectroscopy (XPS). XPS provides a measure of the elemental composition of the fiber surface, along with the respective bonding types. This is done by exposing the sample surface to x-rays, which can eject electrons from their orbitals within an atom. The

kinetic energy of these electrons is proportional to their respective orbitals, and can be detected with a sensor. The energies of these various orbitals can be correlated to the elemental composition of the sample. In this case, XPS was used to identify the chemical bonds present on the fiber surface to determine the level of activation of the carbon fibers. This surface chemistry dictates the bonds that may form with a polymer matrix. These bonds become particularly important for short fiber composites, in which fiber pullout is a critical component of composite failure.

This characterization was carried out using a Kratos AXIS Ultra X-ray Photoelectron Spectrometer. The spectrometer was equipped with a monochromatic Al Kα source operating at 300 W, with a base pressure of 2×10^{-10} torr and an operating pressure of 2×10^{-9} torr. High resolution spectra were taken of the C1s, N1s, and O1s peaks at 20 eV.

The XPS results of the non-sized and sized fibers, as seen in Figure 7 and Figure 8, respectively, indicate that the sizing process increases the quantity of active groups on the fiber surface. The relative percentage of O1s bonds increased from 12.1% to 18.5% due to the applied sizing. The C-OH bonds and C-O bonds also increase from 59.8% to 74.3%, and 11.1% to 37.6% (relative percent), from non-sized to sized fibers, respectively. These groups are available to bond to the amine groups of epoxies, and therefore are expected to increase the interfacial shear strength in the sized fibers [35-37].

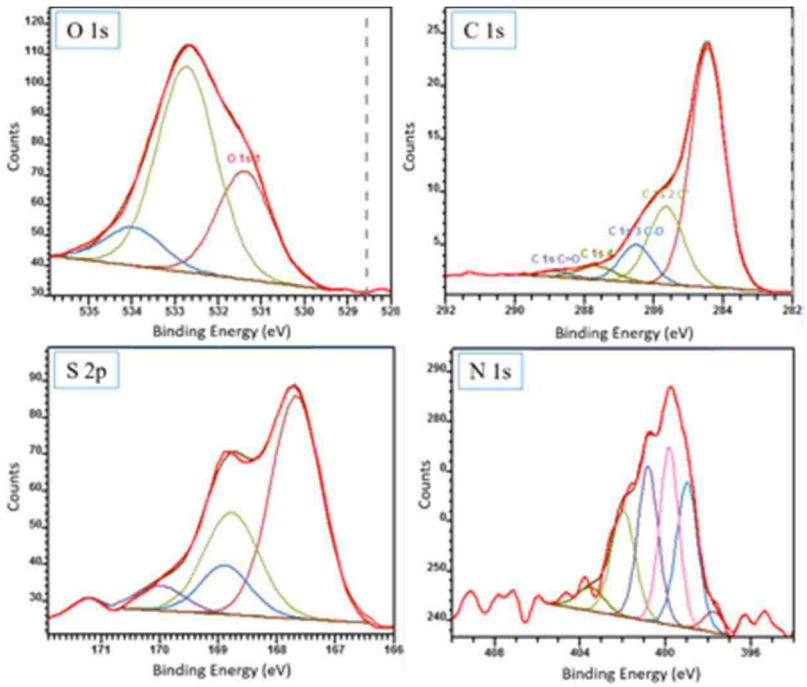

Figure 7 Results of non-sized recycled carbon fiber x-ray photoelectron spectroscopy

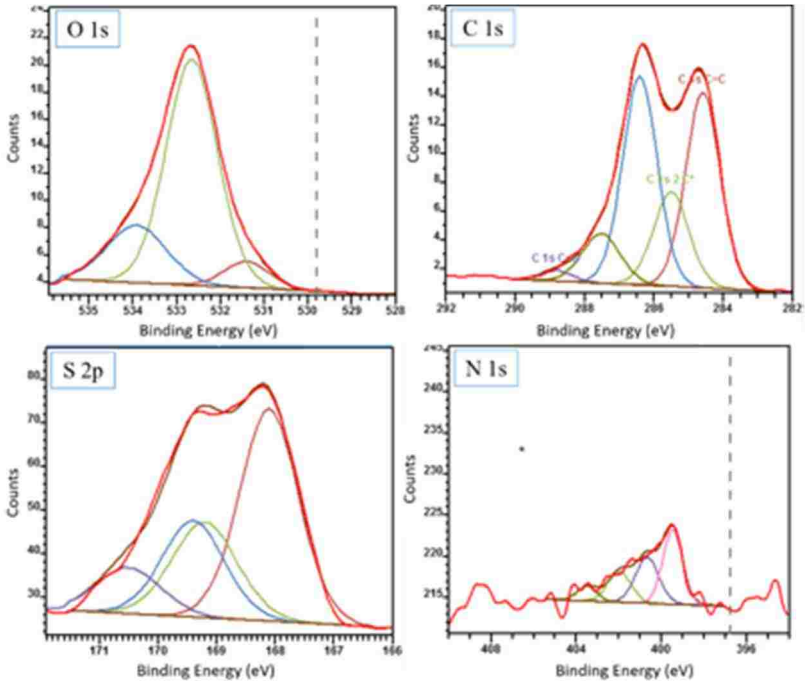

Figure 8 Results of sized recycled carbon fiber x-ray photoelectron spectroscopy.

2.3.3 Single Fiber Fragmentation Test

The interfacial shear strength, τ_{IFSS}, of the carbon fiber was characterized using the single fiber fragmentation test. The method for this test followed the procedure detailed by Feih et al. [38]. In this test, a single carbon fiber is placed in a polymer matrix and a tensile stress is applied to this sample. As the polymer specimen begins to deform, the stress is transferred between the polymer matrix and the brittle fiber reinforcement, which causes the fiber to fracture. As the strain is increased, the number of fractures along the length of the fiber also increases. Once the fiber length drops below the critical length, l_c, the maximum stress that can be transferred to the fiber is lower than the ultimate tensile strength of the fiber, and it will cease to fracture the fiber any further. Any fiber that is above the critical length will fracture, leaving fiber fragments with lengths between l_c and $l_c/2$ at the end of the fragmentation test. If a normal distribution is assumed in this range, the critical length can be found with the expression $l_c = \left(\frac{4}{3}\right) * \bar{l}$, where $\bar{l}$ is the average fiber length [39]. The critical length can then be used to find τ_{IFSS} using the fiber strength, σ_f, diameter, d, and critical length, as seen in Equation 4.

$$\tau_{IFSS} = \frac{\sigma_f}{2}\left(\frac{d}{l_c}\right) \tag{4}$$

In this test, dog-bone shaped tensile specimen nylon molds were 3D printed with a MarkForged Mark 2 printer (no reinforcement fiber) as seen in Figure 9.

Figure 9 3D printed nylon molds for single fiber fragmentation tests. Inset image shows CAD design of mold.

A small notch was included at each end of the mold to allow for a small thread to connect the single carbon fiber to a mass for fiber pre-straining. A length of thread was attached to a small square of cardstock with a cyanoacrylate adhesive, and a single carbon fiber was attached to the other end of the cardstock with the same adhesive (Figure 10). The threads and cardstock pads were used due to the short length of recycled fibers. For longer fibers, the fiber itself can be directly attached to the weight. A 5g mass (exerting a 2 GPa stress on the recycled fibers, which is lower than their ultimate strength, i.e., ~4GPa) was then suspended from each thread to apply a pre-strain before epoxy was added to the mold. The pre-strain is necessary as residual thermal stresses introduce a compressive strain in the fiber, and thus the fiber requires a higher strain to reach its saturation limit [40]. This test was performed on both sized and non-sized fibers using an Aeropoxy PR2032/PH3660 epoxy. The epoxy was degassed under vacuum for a

minimum of 30 minutes before being added to the molds. The molds were allowed to cure for 24 hours, after which a post-cure was performed at 80 ℃ for two hours.

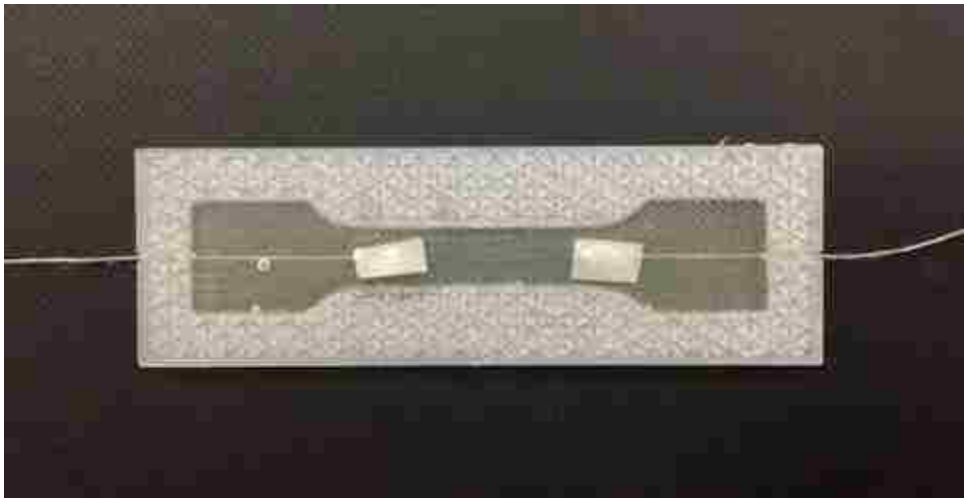

Figure 10 Molded single fiber fragmentation test specimen. A 7.5g mass was suspended from each thread protruding from the mold prior to curing.

The samples were strained until fracture, typically up to roughly 2% strain, at a displacement rate of 0.05 in/min in an Instron tensile testing device. The samples were then observed under with an AmScope microscope using cross-polarized light to view birefringence patterns along the sample at the points of fiber fracture. These patterns make the fiber fractures easy to identify and analyze. Examples of the observed birefringence patterns are shown in Figure 11.

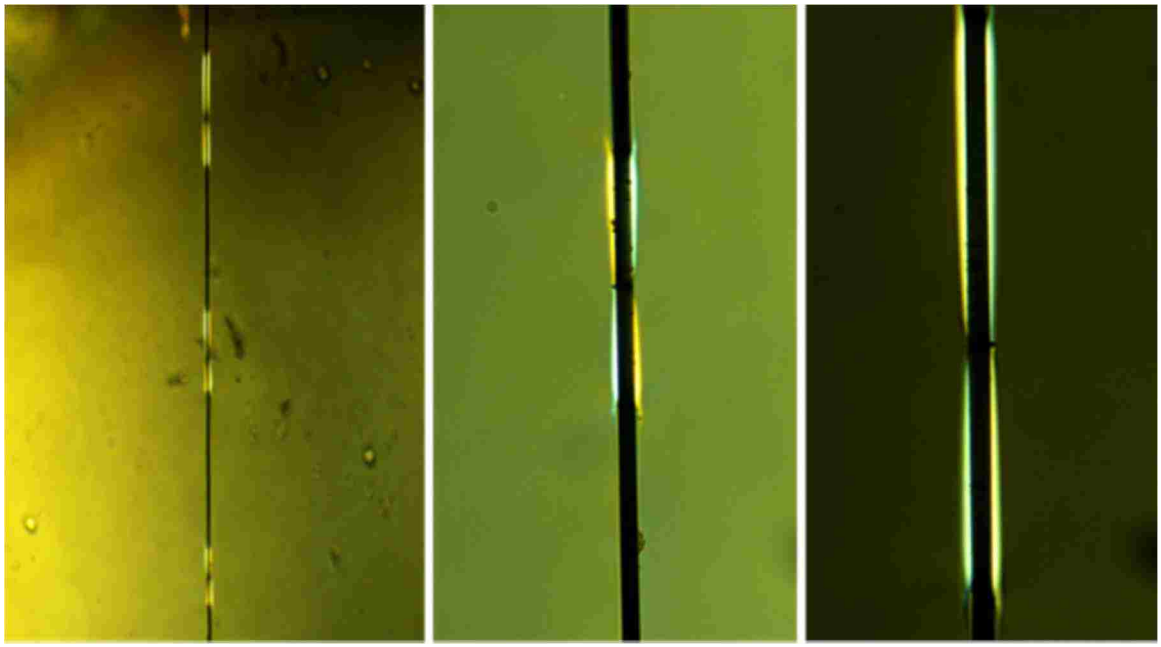

Figure 11. Birefringence patterns on fractured sized recycled carbon fiber

The single fiber fragmentation results in this study were inconsistent, and need further research to be determined precisely. A few factors are thought to be responsible for the lack of consistent results. For one, the epoxy used in this study has a failure strain of 1.76%, which is thought to be too low to achieve fracture saturation of the fiber. Additionally, the printed molds impart a pattern on the epoxy corresponding to the mold roughness, which causes optical distortions when viewing the fibers. Future studies will incorporate a more ductile epoxy system, along with careful grinding and polishing of the sample to achieve a smooth, flat, and thin sample before imaging.

In general, increasing the percentage of activated carbon on the fiber surface leads to an increase in interfacial shear strength, though this is not always the case. Yao et al. found that the IFSS of fibers with 10.32% activated carbon was approximately 60 MPa, while fibers with 39.86% activated carbon had an IFSS of roughly 77 MPa with an epoxy matrix [41]. Additionally, as the activated carbon on the fiber surface was increased, a

corresponding increase in IFSS was observed. The activated carbon on the fiber surface in this study was found to increase from 21.6% to 53.3% (atomic%) from the non-sized to sized fibers. This is compelling evidence that the fibers have been effectively sized, and are likely to exhibit a high interfacial shear strength.

Jiang et al. also found that a reduction in surface oxygen resulted in a reduction of interfacial shear strength for recycled fibers. The pyrolysis recycling process used was found to reduce the O/C concentration ratio from 0.258 to 0.189. The recycled fibers also experienced a reduction in the IFSS with epoxy from 82.5 MPa with virgin fiber to 64.2 MPa with recycled fiber. The sizing process used in this study increased the O/C ratio from 0.143 to 0.232, which again is expected to increase the interfacial shear strength of the fiber/epoxy system. [20]

Another possible explanation for the discrepancy in the fragmentation test results is that the short length of examined fibers, i.e. ~1 cm, is similar to the fiber critical length. Theoretical modeling results, shown in Chapter 5, suggest a relatively low interfacial shear strength in rCFRP composites and thus a relatively long critical fiber length of ~4 mm. It is, however, unclear why the activated rCF surface did not bond strongly to the polymer matrix.

2.4 Mechanical Characterization

2.4.1 Single Fiber Tensile Test

The mechanical properties of the recycled carbon fibers were investigated using single fiber tensile tests. These tests were performed in accordance with the ASTM C1557-14 standard, using a specimen gauge length of 1/2". A 1/2" square punch was used to remove a window out of thick index paper, across which the carbon fiber was placed (Figure 12). The ends of the fibers were attached to the paper using a cyanoacrylate adhesive, and subsequently gripped with a tensile testing device. The sides of the window were carefully cut prior to the test, leaving only the fiber between the clamps. The device used for these tests was a TA instruments DMA Q800, equipped with film tension clamps, with a strain resolution of 1 nanometer. A displacement ramp of 1200 µm/min was applied until sample failure. A minimum of 20 fibers were tested for a

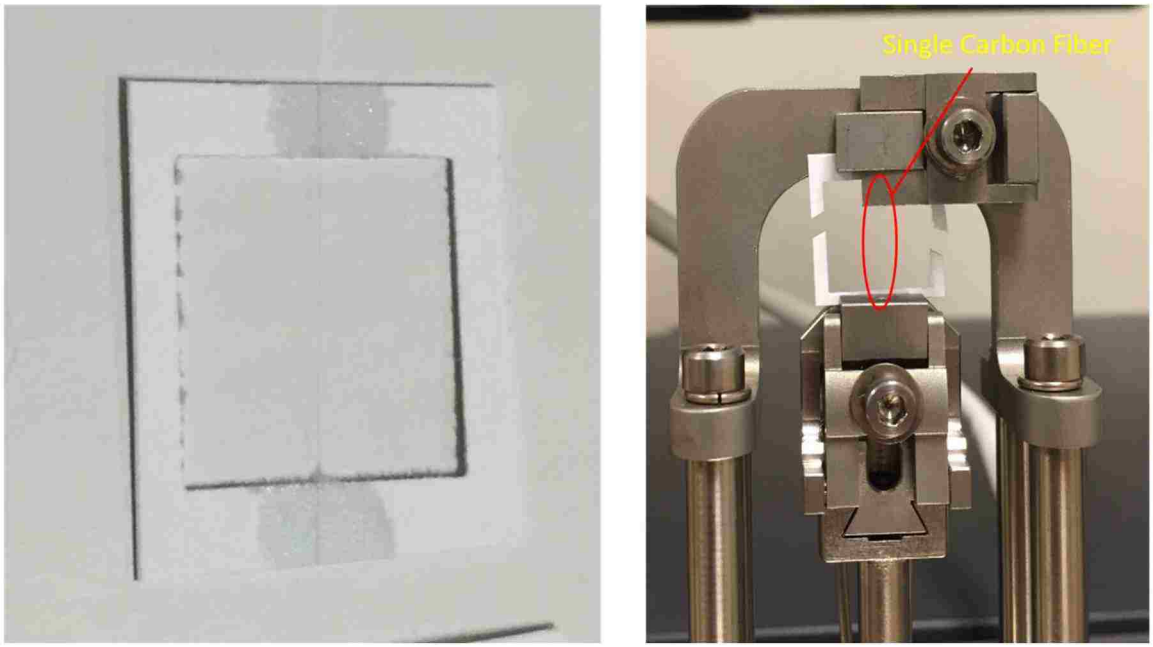

Figure 12 Single fiber tensile sample and experimental setup

given sample.

The device was calibrated prior to testing with force, position, and clamp calibrations. The module “DMA Strain Rate” was used, with the method “Displacement Ramp.” A static force of 0.0010 N was applied, with a specified initial displacement of 0 μm. The samples typically fractured in under ten seconds. A representative sample of the tensile test data is illustrated in Figure 12. This sample has a tensile strength of 3023 MPa, a tensile modulus of 251.8 GPa, and a strain-to-failure of 1.2%.

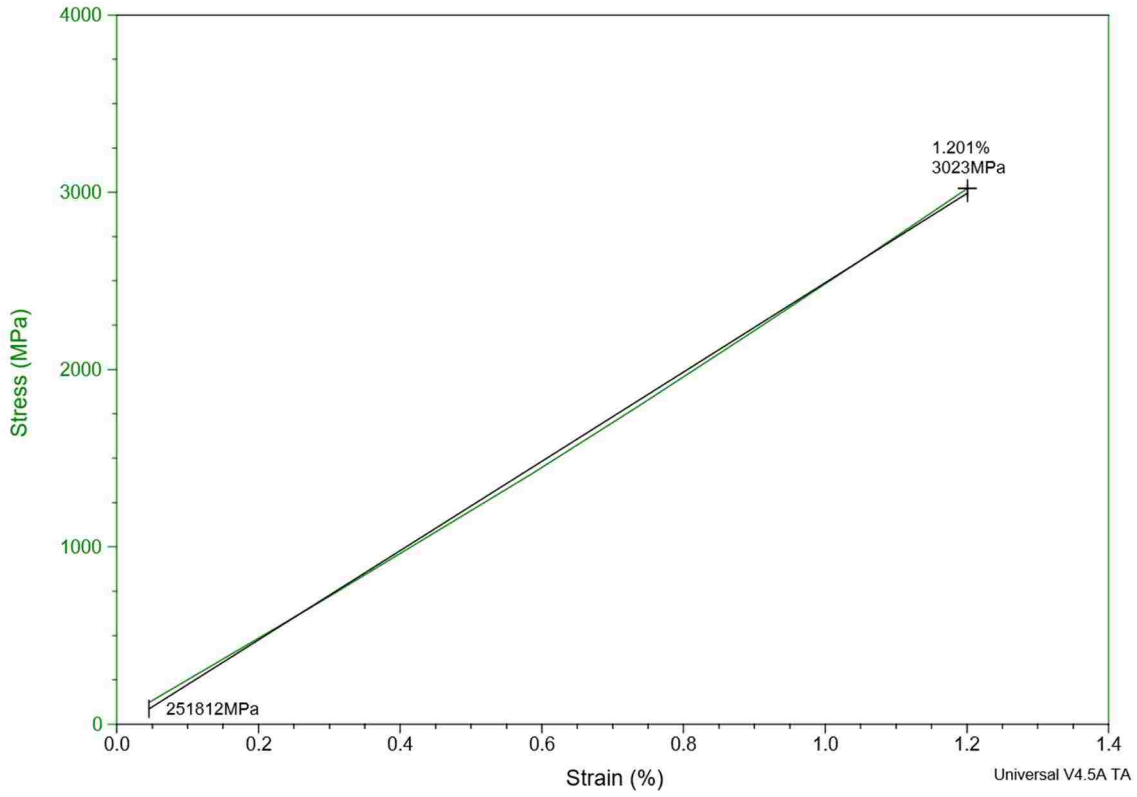

Figure 13 Representative single carbon fiber tensile stress-strain curve

.

The tensile strength and modulus for non-sized recycled fibers is shown in Figure 13. The average strength and modulus for the non-sized recycled carbon fibers was 3828 MPa and 313.4 GPa, respectively, with standard deviations of 17 and 19%. The average strain to failure of these carbon fibers was 1.21%, with a standard deviation of 15%. The recycled composite source of these fibers contained T800 carbon fibers, which have a reported strength and stiffness of 5490 MPa and 294 GPa, respectively [24]. Therefore, the recycled fibers have a reduction in strength of roughly ~25%, with a comparable modulus to virgin fiber.

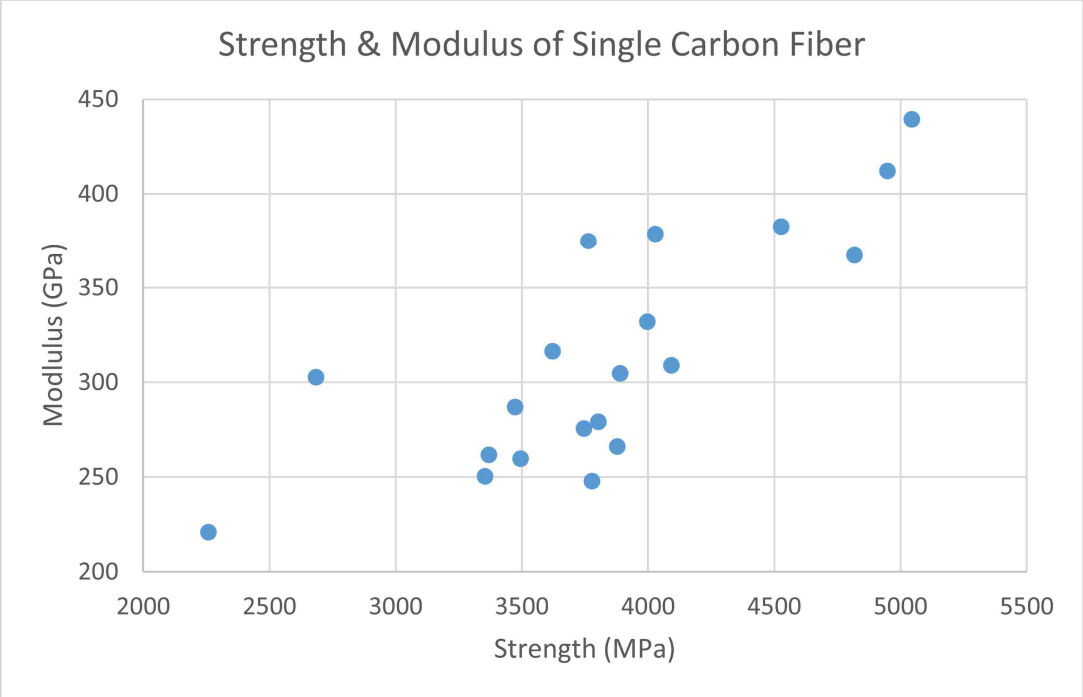

Figure 14 Tensile strength and modulus measured for single non-sized carbon fibers.

2.4.2 Weibull Analysis

A Weibull analysis was applied to the single fiber tensile data results. Weibull analysis operates on the assumption that the most critical flaw will initiate specimen failure, which is appropriate for brittle fiber analysis [42]. The Weibull model describes the probability of fiber failure with Equation 1.

$$P(\sigma_f) = 1 - \exp\left\{-\left(\frac{V}{V_0}\right)\left(\frac{\sigma_f}{\sigma_0}\right)^m\right\} \quad (1)$$

In this equation, $P(\sigma_f)$ is the probability of fiber failure, V_0 is the reference gauge volume, V is the fiber volume, σ_0 is the scale parameter, and m is the shape parameter. When the volume is assumed constant, as with brittle materials, Equation 1 can be rearranged to obtain Equation 2.

$$ln\left(-ln\left(1 - P(\sigma_f)\right)\right) = mln(\sigma_f) - mln(\sigma_0) \quad (2)$$

The probability of fiber failure, $P(\sigma_{f_i})$, can be estimated for each sample tested by sorting the failure strengths in ascending order, where i=1 corresponds to the lowest failure strength and i=n corresponds to the highest failure strength, and using the approximation illustrated in Equation 3.

$$P(\sigma_{f_i}) = \frac{i - 0.5}{n} \quad (3)$$

For this study, 20 fibers were tested (n=20). The assumption used for $P(\sigma_{f_i})$ in Equation 3 can then be inserted in Equation 2 and a plot can be generated. A least squares regression fit can be used with this data to find m and σ_0. This analysis was used for both

the stress and strain results of the tensile data. Once the shape parameter and scale parameter have been found, the probability of failure can be plotted against stress using Equation 3. The scale parameter represents the maximum strength that the weakest 63% of fibers in a population will display, and therefore is often reported as the tensile strength of the fibers tested [10].

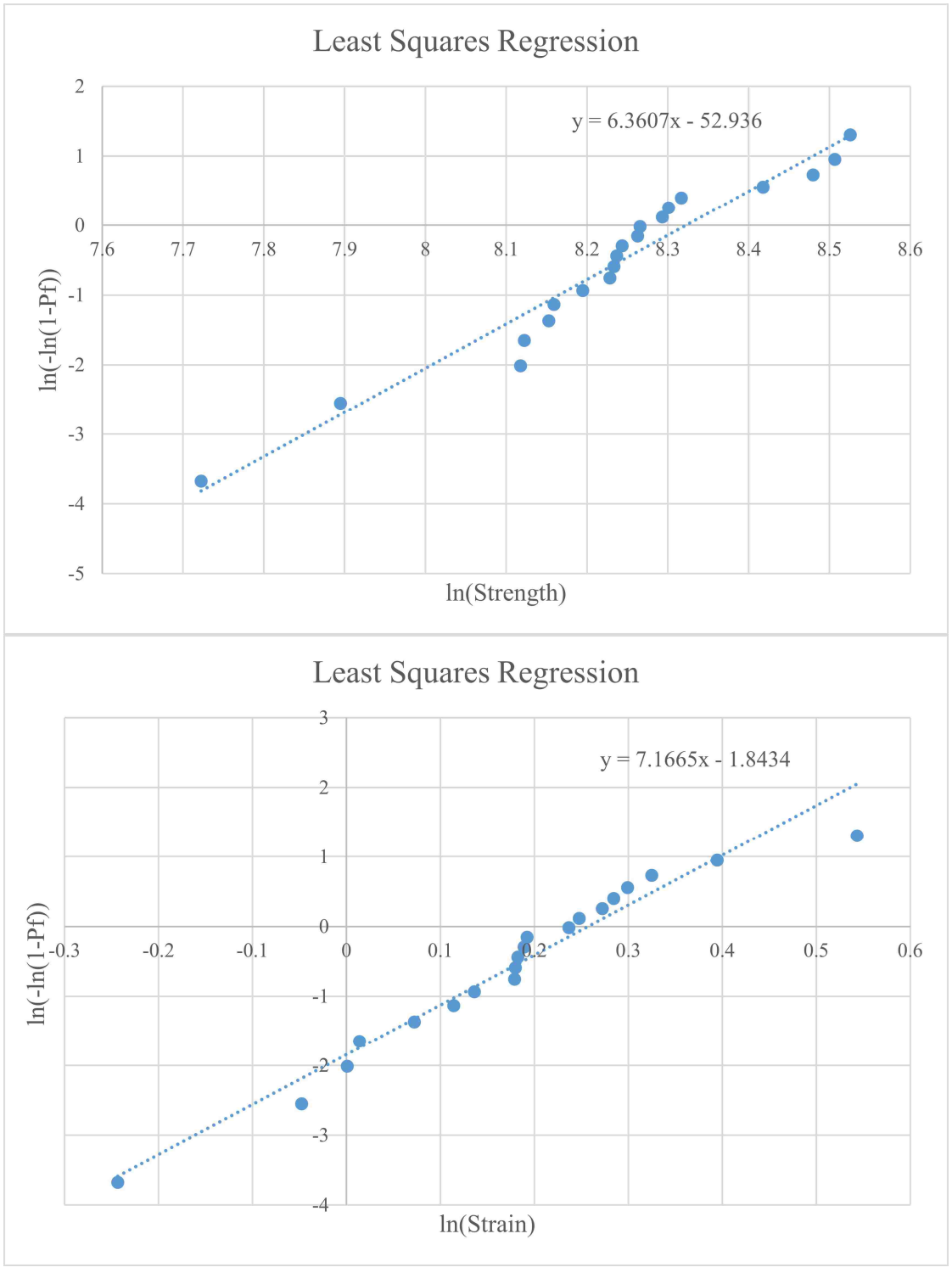

Figure 15 Weibull analysis of stress and strain for single non-sized recycled carbon fiber

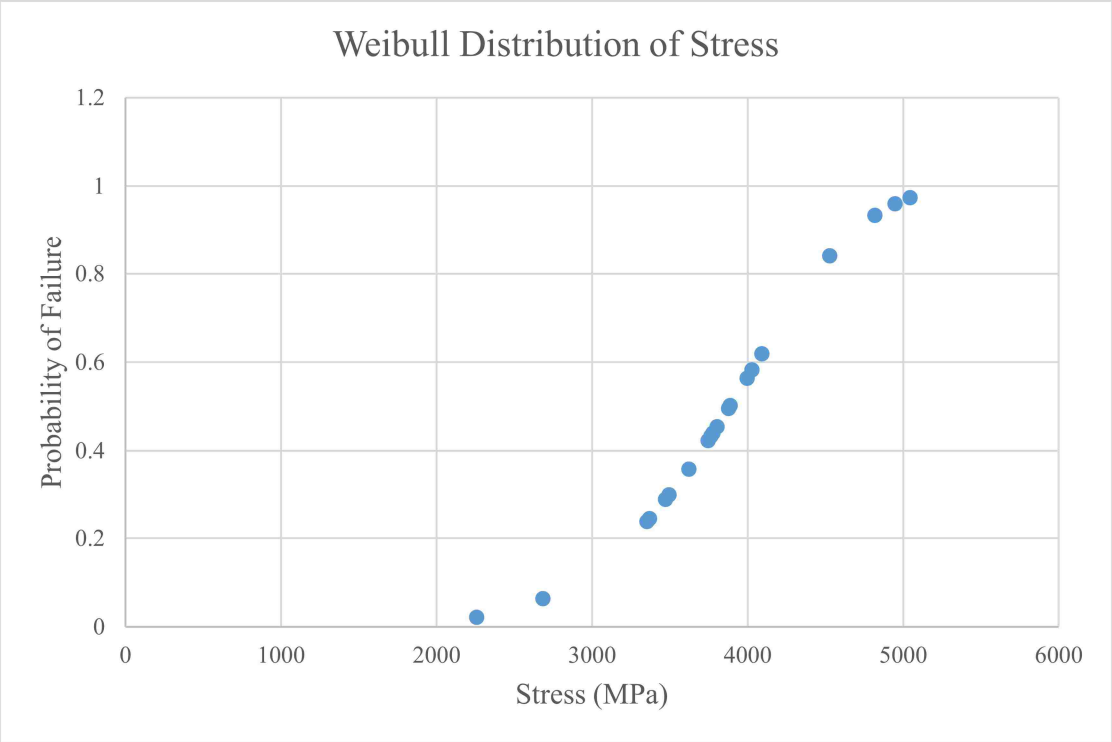

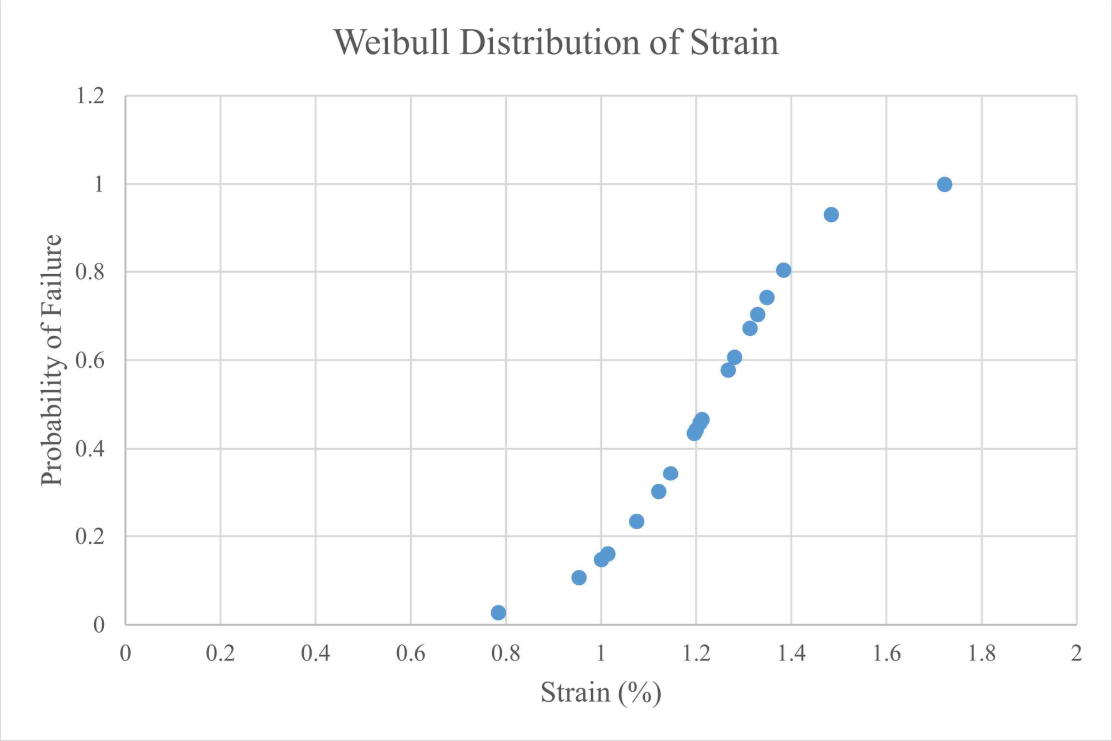

Figure 16 Weibull distributions for stress and strain of non-sized recycled carbon fiber.

The Weibull analysis and distribution for the single fiber tensile tests are shown in Figure 15 and Figure 16, respectively. The mechanical properties of the fibers are summarized in Table I. A least squares regression was used to determine the Weibull shape and scale parameters. The probability of failure was then plotted as a function of applied stress and strain. While the modulus was unaffected by the recycling process, the strength experienced a 25.2% reduction.

Table I. Summary of single fiber mechanical properties.

	Strength (MPa)	**Modulus (GPa)**
Recycled Fibers (experimentally measured values)	4115	313.4
Virgin T800H Fibers [43] (manufacturer values)	5500	294
Retention of Properties	74.8%	100%

Chapter 3. Remanufacturing Recycled Carbon Fiber Composites

3.1 Non-aligned Carbon Fiber Mats

3.1.1 Manufacturing Process

In-plane randomly oriented recycled carbon fiber mats were fabricated as seen in Figure 17. The recycled fibers were first dispersed with an axial impeller in a glycerol and water solution (19:1 wt/wt) until only single fibers and small bundles exist. The viscous solution allows for higher shear forces, which disperse fibers much more effectively than lower viscosity mediums. Typically, 500 mg of fibers were dispersed in 200 ml of glycerol at 1100 rpm for 5 minutes. Any large bundles were removed from the solution, and the solution was poured over a nylon mesh covering an 8" sieve. This process was repeated until a total of 10g of carbon fiber were deposited. A vacuum was pulled after each new addition of fibers to remove glycerol and densify the mat. After a 10g of fibers were deposited, the mat was thoroughly rinsed with warm water and dried at 180 ℃ for two hours.

Figure 17 Non-aligned mat production process involving dispersion of recycled fibers into viscous glycerol solution and deposition of fibers onto nylon covered sieve.

3.2 Aligned Carbon Fiber Mats

Processing of the aligned recycled carbon fiber composite can be broken down into three steps. First, the entangled fiber clumps were dispersed in a viscous medium down to the single fiber level, without significantly damaging the fibers but shortening them in length. Next, these fibers were deposited onto a nylon mesh with preferential orientation, in this case using a velocity differential and convergent nozzle. Lastly, the viscous medium was fully removed, and the mat was thoroughly rinsed and dried. Various parameters affect the success of each step, and will be discussed in detail.

3.2.1 Manufacturing Process

The viscous medium used to disperse the carbon fibers is a glycerol solution, mixed to approximately 96 wt% glycerol and 4 wt% deionized water. This mixture gives a resulting viscosity of 624 centipoise at 20 ℃, and 281 centipoise at 30 ℃ [44]. For comparison, water at 20 ℃ and 30 ℃ has a viscosity of 1.005 and 0.8007 centipoise, respectively [44]. This high viscosity is necessary to provide the shear force required to separate clumps of carbon fiber when using an axial impeller.

The overall setup of the alignment rig is shown in Figure 18. The carbon fiber slurry was prepared by adding approximately 60-100 mg of carbon fiber to 500 ml of glycerol solution. This solution was mixed with an axial impeller at 1100 rpm for 5 minutes. The impeller was placed near the edge of the mixing container, in this case a 1 liter funnel, to maximize shear forces in the region between impeller and container wall. Within the funnel, larger bundles of fibers were trapped in the fluid vortex while dispersed fibers travelled with the glycerol out of the funnel.

When the fiber slurry exits the funnel, it travels through a flexible tube toward a converging nozzle. The tube is attached to a reciprocating rack, which travels on a single axis according to an alternating positive and negative constant velocity over a five inch distance. The convergent nozzle is placed inside of a rotating mesh drum, with the nozzle velocity aligned along the drum axis. The fibers become partially aligned as they exit the nozzle, and are further aligned as they contact the mesh on the drum. The shear flow in the convergent nozzle partially aligns the fibers and the mismatch in velocity between the fiber jet and drum rotation causes the bottom of the fiber to be 'pulled' along the circumference of the drum, thus aligning the fibers in this direction.

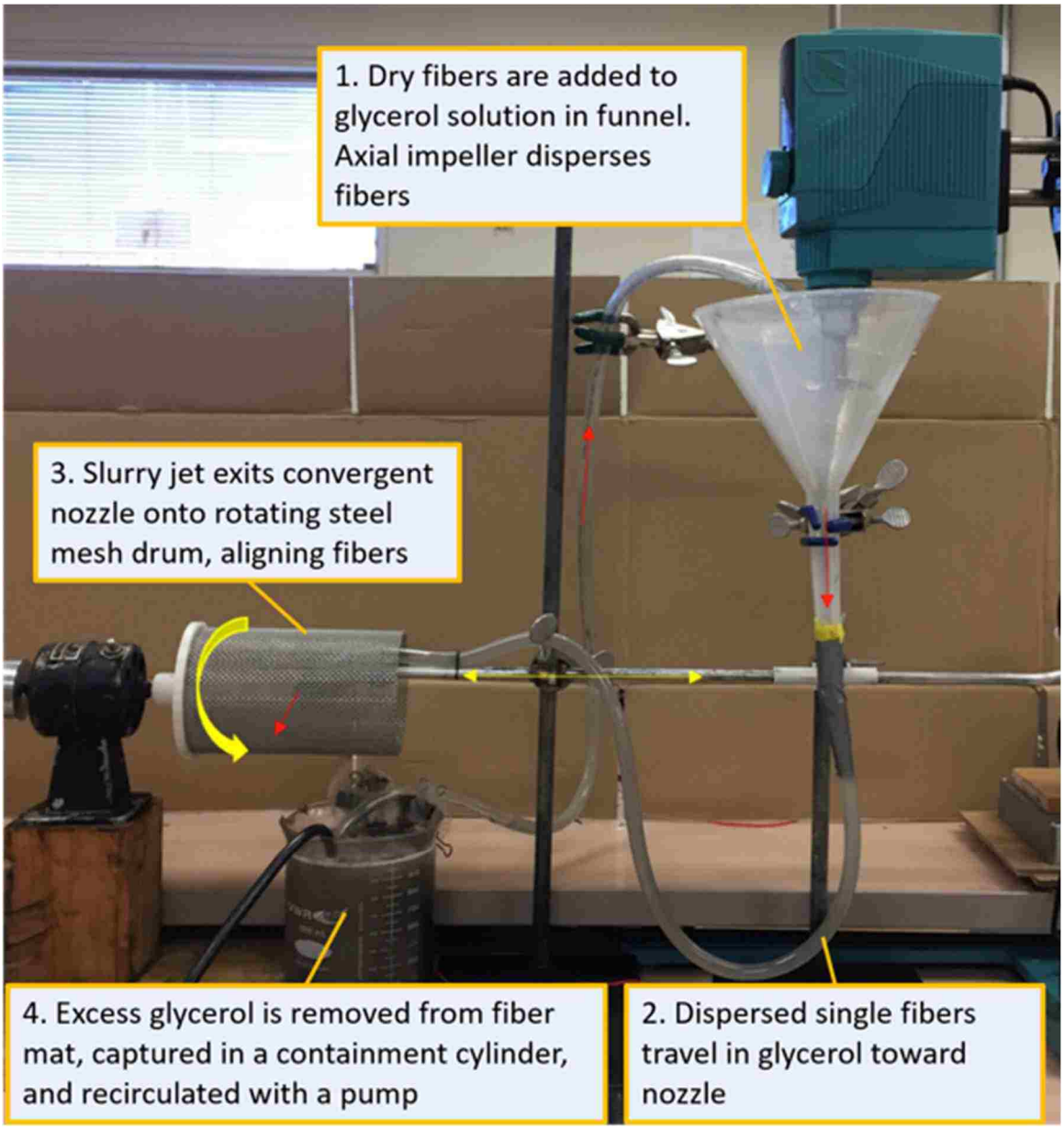

Figure 18. Centrifugal alignment rig. Red arrows indicate direction of fluid flow, yellow arrows indicate mechanical motion.

The length, width, and thickness of the resulting aligned mat is determined by the drum diameter, maximum nozzle travel, and amount of fibers deposited, respectively. The drum is made from a rolled piece of 6"x12" stainless-steel wire cloth, with a 0.032"

wire diameter and a 0.051" opening size (37.5% open area). However, the carbon fibers do not tend to adhere well to the steel, so a thin nylon mesh is inserted to cover the inside of the drum. This also allows for simplified removal of the aligned mat once the desired thickness is achieved. An example of an aligned mat produced with this technique is shown in Figure 19.

Figure 19. 1.5g mat of aligned recycled carbon fibers, approximately 5"x10". The red arrow shows the fiber alignment direction.

To ensure that the processing of carbon fibers into aligned mats did not degrade the fiber length beyond the critical length, a length distribution of fibers was found through microscopy. For this experiment, a random selection of fibers was taken from a processed, rinsed and dried rCF mat and dispersed across a piece of white cardstock. Once the fibers were spread out enough to allow for individual length identification, a picture was taken of roughly a 2"x2" square area. The fibers were traced with image

analysis software (ImageJ) to measure their length. Over 500 fibers were measured with this technique, and the length distribution is shown in Figure 20.

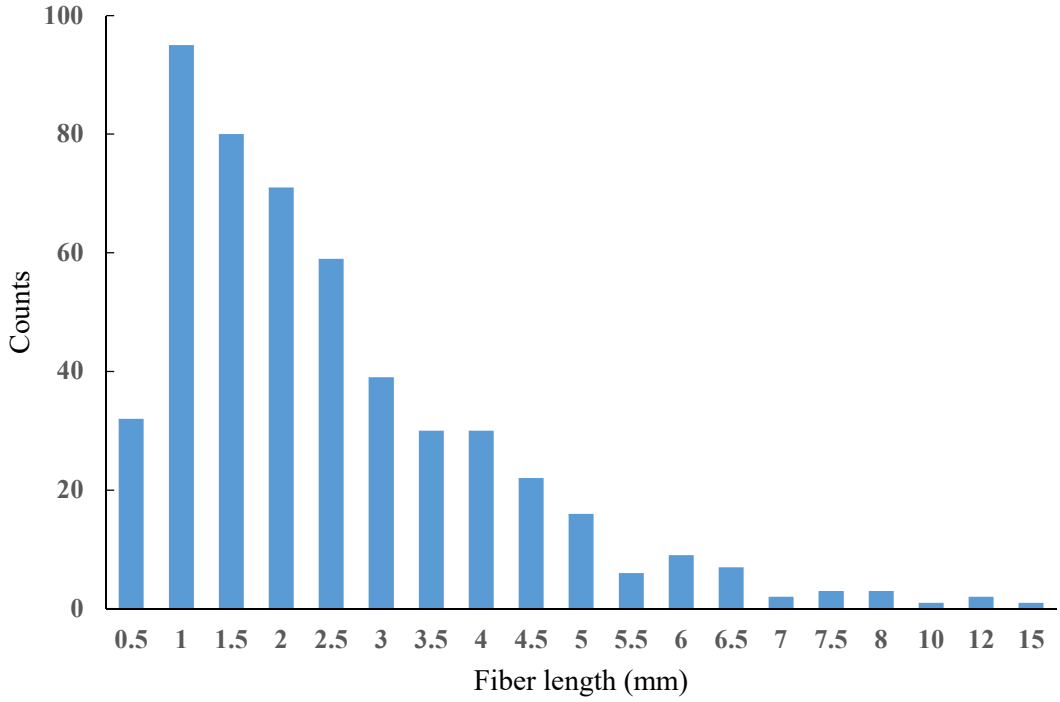

Figure 20. Recycled carbon fiber length distribution after processing.

3.2.2 Alignment Characterization

The degree of fiber alignment in the mats was quantified prior to composite manufacturing using light microscopy and the image analysis software ImageJ with the plug-in FibrilTool. FibrilTool describes the degree of anisotropy in an image, and was developed specifically to quantify the degree of alignment of fibrillar systems [45]. The software analyzes pixel intensities as a function of 2D coordinates and produces an anisotropy score that lies between 0 and 1, with 0 being completely random and 1 being completely aligned.

Thin sections of the carbon fiber mat were placed between two clean glass slides, and pressed together with small binder clips. This was necessary to force the fibers into a single plane for higher quality images. The dark field images were taken at 10x magnification. The images were then processed with ImageJ to increase the contrast of the fibers with respect to the background, and were eventually converted to binary for ease of orientation detection. At this point, the region of interest for FibrilTool was selected as the maximum area of the image that was in focus, and the degree of anisotropy was calculated. As a reference, virgin aligned carbon fiber was also analyzed. An example of the image processing and analysis of the aligned virgin fiber, non-aligned recycled fiber, and aligned recycled fiber can be seen in Figure 21.

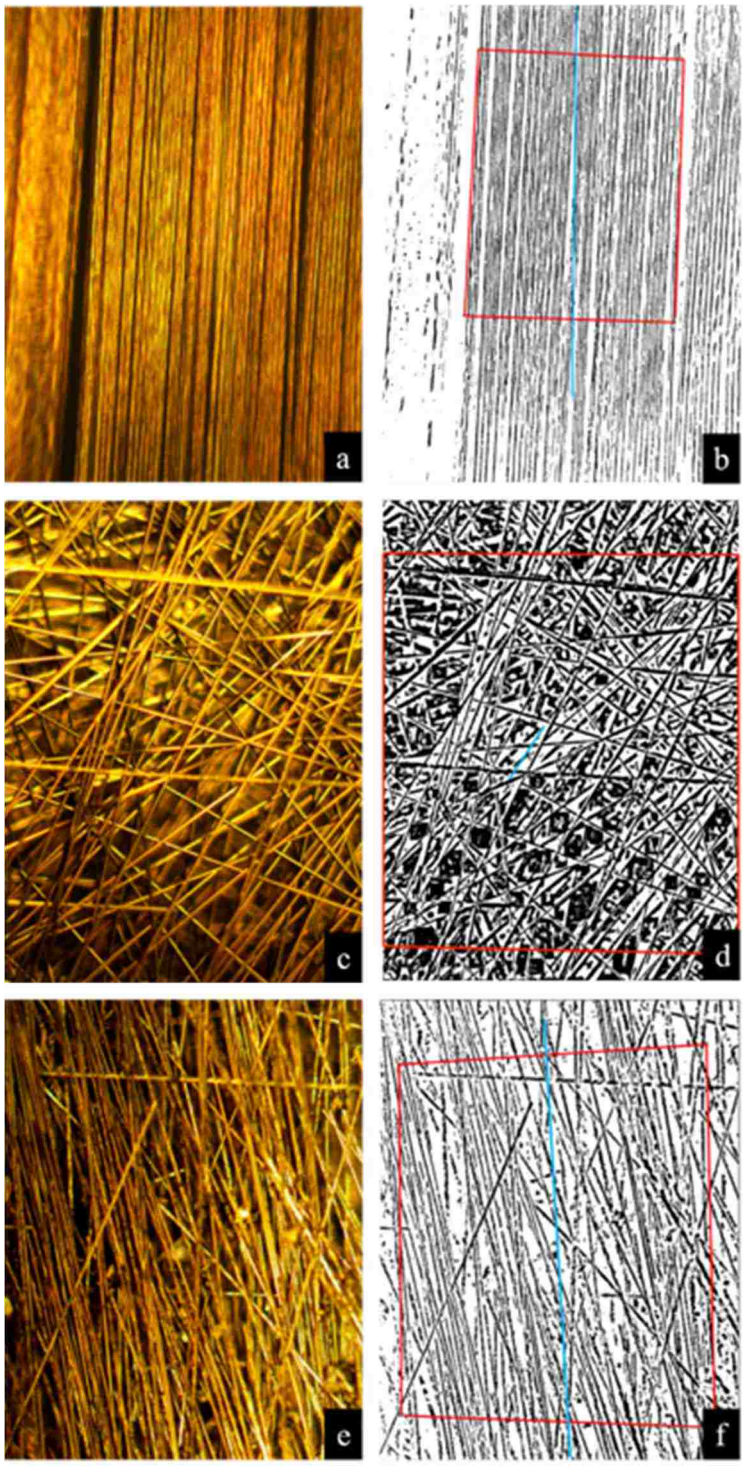

Figure 21. Raw dark field (DF) images (left) and processed images (right) for aligned virgin fiber (a,b), non-aligned recycled fiber (c,d) and aligned recycled fiber (e,f). The red box defines the ROI, the direction of the blue line is the average fiber direction, and length of the line corresponds to degree of anisotropy

The alignment was also characterized by tracing all the fibers in an image and measuring the fiber angles with ImageJ. The front and back of two samples with differing anisotropy scores were measured, and histograms of the fiber orientation were created. In each case, a minimum of 100 fibers were measured. The fiber orientation distributions of an aligned mat processed without optimal parameters are shown in Figure 22 and Figure 23, corresponding to the back and front of the mat, respectively. The back and front of this mat were found to have anisotropy scores of 0.3200 and 0.3571, respectively. The fiber angle distribution shows that 39.4% and 67.9% of the fibers on the back and front of the mat, respectively, fall within ±15 degrees of the mean. Figure 25 and Figure 24 show the alignment distribution of a fiber mat that was processed with the optimal conditions found in the two-factorial experiment. This mat was found to have anisotropy scores of 0.5579 and 0.4011 on the back and front of the mat, respectively. For this sample, 72.6% and 66.4% of the fibers fall within 15 degrees of the mean angle for the back and front of the mat, respectively.

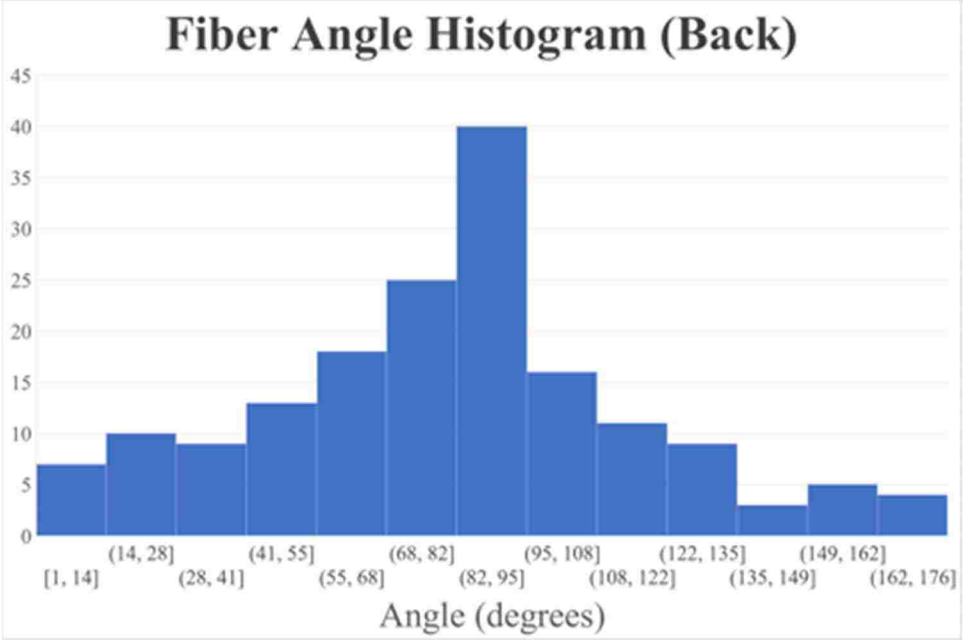

Figure 22 Fiber orientation histogram of the back of aligned mat before parameter optimization, with a corresponding anisotropy score of 0.3200

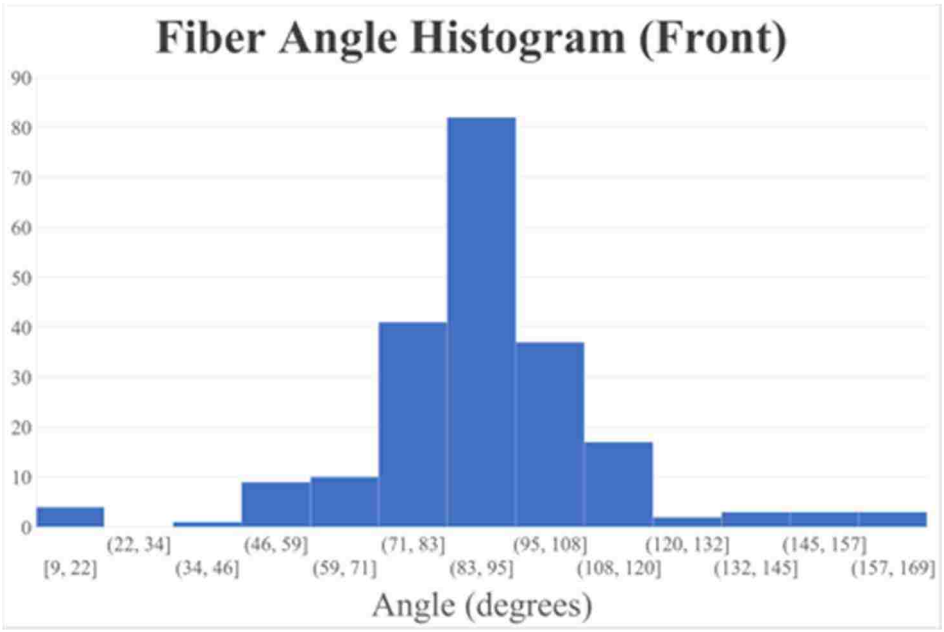

Figure 23 Fiber orientation histogram of the front of aligned mat before parameter optimization, with a corresponding anisotropy score of 0.3571

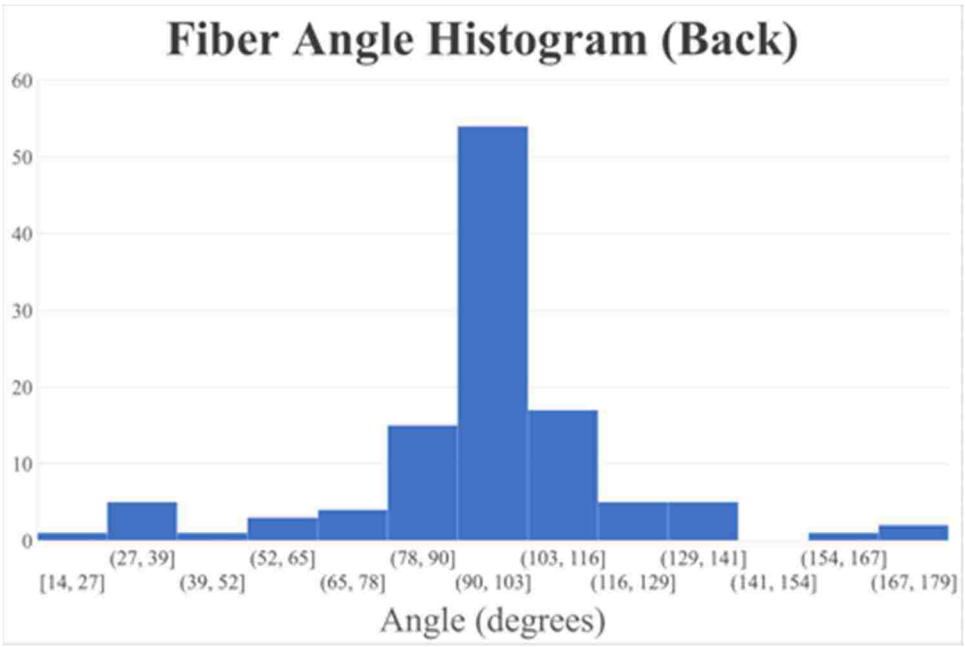

Figure 25 Fiber orientation histogram of the front of aligned mat after parameter optimization, with a corresponding anisotropy score of 0.5579

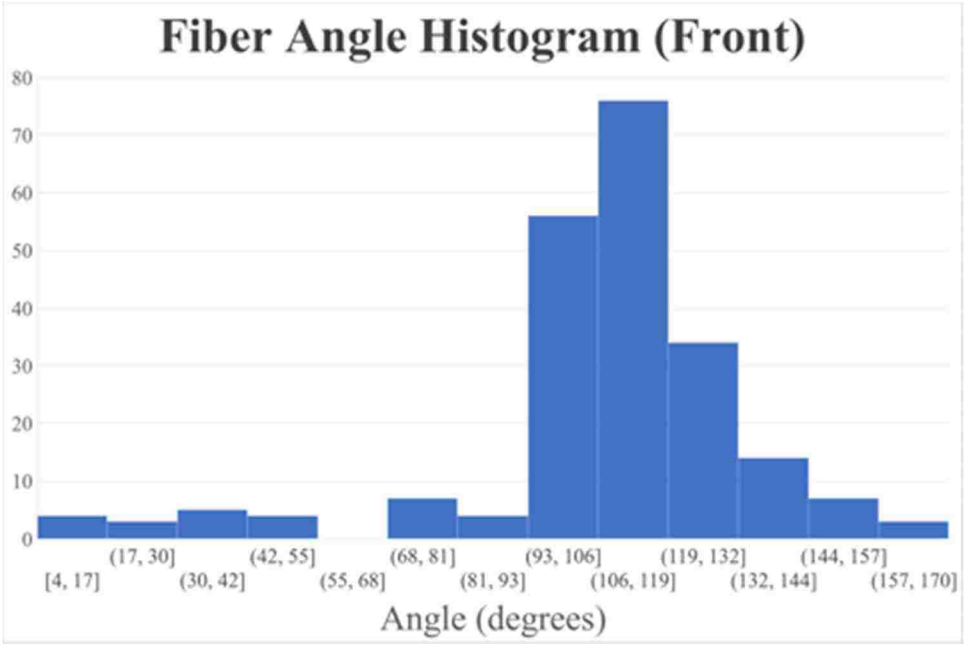

Figure 24 Fiber orientation histogram of the front of aligned mat after parameter optimization, with a corresponding anisotropy score of 0.4011

3.2.3 Two Level Factorial Experiment

The parameters that are thought to most affect fiber alignment, based on experimental observations, are given below.

- Reciprocating rack velocity
- Solution viscosity
- Mat thickness
- Drum rotational velocity

These parameters were optimized using a two-level factorial experiment, in which 8 carbon fiber mats were produced. Each mat had a unique combination of experimental parameters, consisting of one of two modes of each parameter. Specifically, these modes consisted of a high and low reciprocating rack velocity, a high and low solution temperature to adjust glycerol viscosity, and a high and low drum rotational velocity. These parameters are summarized in Table 2. In general, it was observed that as the thickness of the mat increased, the degree of the alignment decreased, due to a decrease in permeability of the mat. It was found that 1.5 g mats were thick enough to maintain their structural integrity during handling, while 1 g mats would easily disintegrate in most conditions. Therefore, a mat thickness of 1.5 g was chosen for the experiments, and was not varied for the two-level factorial experiment.

Table 2. Two level factorial design parameters.

Parameter	High (+)	Low (-)
Reciprocating Rack Velocity	2 in/sec	1 in/sec
Solution Temperature	30 ℃	25 ℃
Drum Rotational Velocity	600 rpm	400 rpm

The alignment on the front and back sides of each mat was quantified by taking an image and using the FibrilTool to measure the fiber anisotropy. As illustrated in Figure 21, the region of interest (ROI) was selected as the largest in-focus area of each image, and anisotropy score was computed. In general, it was found that the back of each mat, corresponding to the last layer of fibers deposited, displayed a lower anisotropy score than the front of the mat (first layer deposited). The anisotropy score was found on both the raw microscopy images as well as the images after processing to be affected by artifacts that exist due to image quality. The settings used for each trial can be seen in Table 3.

Table 3 Settings used for each trial in the two-factorial experiment

Trial	Linear Velocity	Solution Temperature	Rotational Velocity
1	+	-	-
2	+	-	+
3	+	+	-
4	+	+	+
5	-	-	-
6	-	-	+
7	-	+	-
8	-	+	+

The results of the two-level factorial experiment are shown in Figure 26. These also illustrate the effect of image processing on the ability of FibrilTool to determine the anisotropy score. The uniformity of each mat was also considered quantitatively. The final design parameters were chosen based on trial 8, which displayed a high anisotropy score for both the processed and unprocessed images.

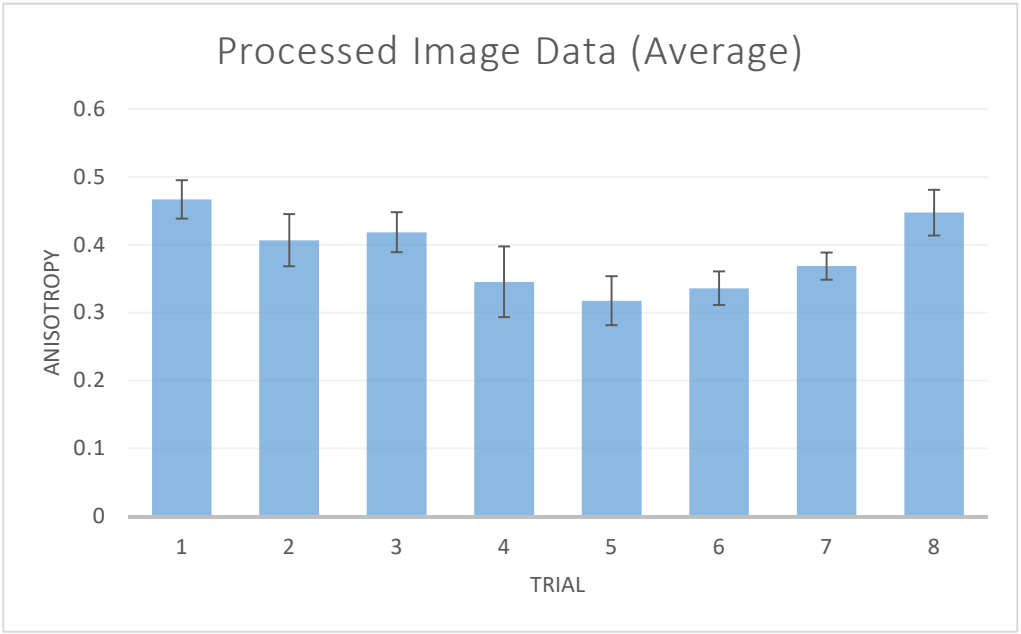

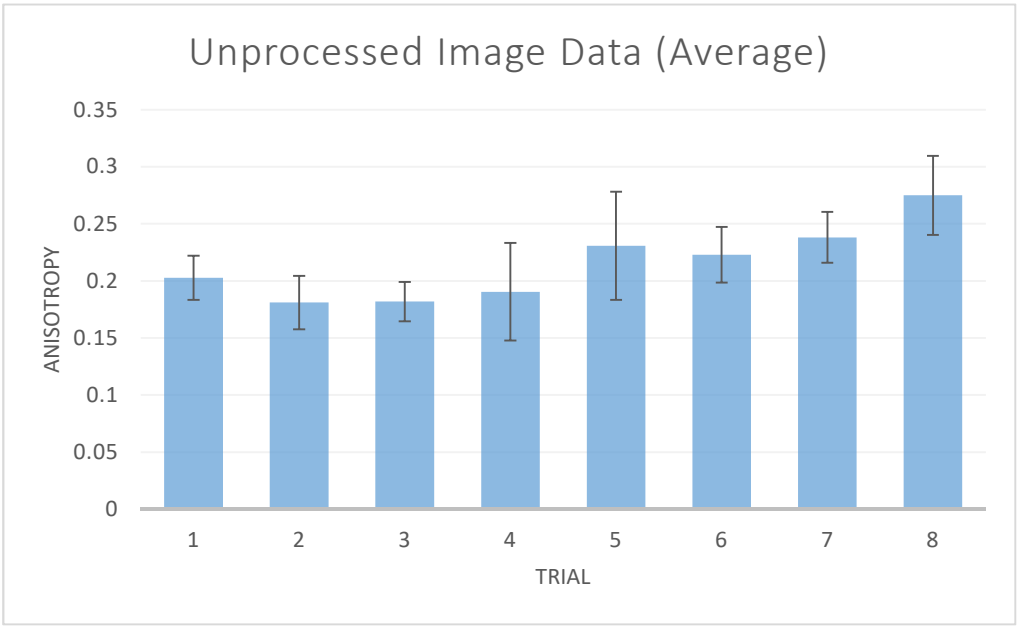

Figure 26 Average anisotropy scores (front and back) taken from processed images (top) and unprocessed images (bottom)

The modes of each parameter which produced the highest quality alignment were selected to produce the mats required for the composite. Specifically, the mats were processed with a low linear nozzle velocity (1 in/sec), a high temperature (30 ℃), and a high rotational velocity (600 rpm). These parameters can be understood somewhat intuitively. A small linear nozzle velocity is required to reduce movement of the fibers in the direction perpendicular to the alignment axis as they are deposited on the mesh drum. However, a sufficiently low linear velocity would cause the solution to deposit on glycerol rich portions of the mesh, which would have had insufficient time for the glycerol to be removed from the mat. The higher temperature creates a much lower solution viscosity, which in turn can permeate through the previous fiber layers as well as nylon and steel meshes more easily. A lower viscosity also reduces the shear force exerted on the fibers during the dispersion process, but this viscosity was not found to significantly hinder the production of a uniform fiber slurry. The high rotational velocity also removes the glycerol solution from the mat and meshes more quickly, and provides a larger velocity differential to encourage a higher degree of alignment. However, at larger rotational velocities the solution would splash as it contacted the mesh, which would nullify any preferential alignment and create highly non-uniform thicknesses. Each composite plate required a minimum of 15g to produce a sufficient volume fraction, which amounted to between 10 and 15 mats. The aligned mats were stacked together, with all fibers oriented along the same axis. These mats were then infused with epoxy in a resin transfer molder (RTM).

3.3 Composite Manufacturing

3.3.1 Resin Transfer Molding (RTM)

The basic layout of an RTM is illustrated in Figure 27. There existed a 1.3 mm gap between the top and bottom of the RTM mold used in this study. The inside of the mold was 12"x12", which was effectively reduced for a 5"x5" sample using 1mm thick rubber cut to outline the sample. Channels were made with this rubber to direct the epoxy to overflow tubes as shown in Figure 27. Once the carbon fiber mats were placed into the mold, the mold was sealed with four 1/2" bolts. The epoxy was mixed and added into the infusion cylinder, which contains a piston connected to an electric motor. The epoxy was degassed for a minimum of 30 minutes. Once thoroughly degassed, a transfer tube was attached to connect the cylinder and the mold. The epoxy was infused at a rate of 2 cc/min, and set to infuse 100 ml of epoxy into the mold. Typically, epoxy would begin to flow out of the overflow tubes after 90-100 ml of epoxy was infused.

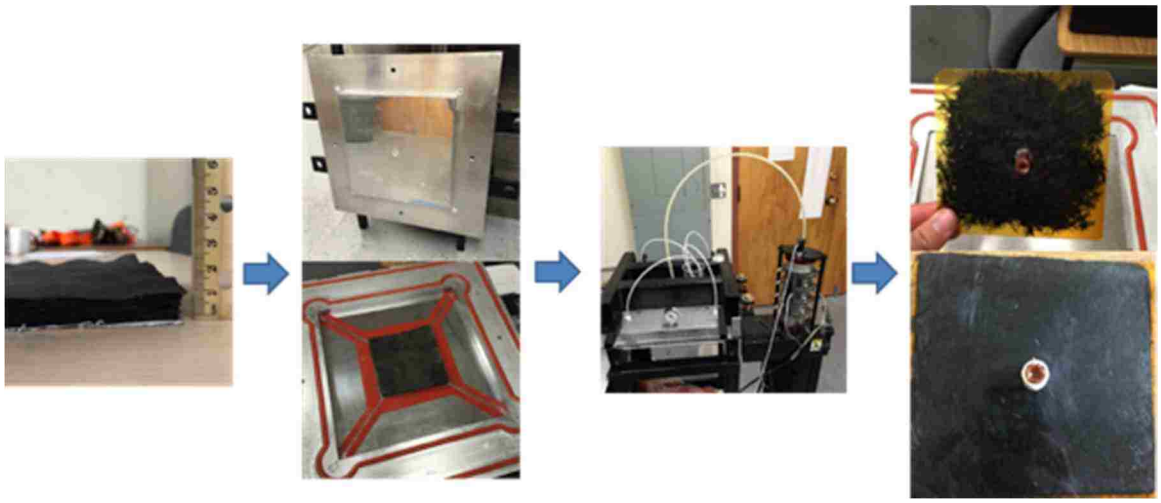

Figure 27. Resin transfer molder used to infuse recycled carbon fiber mats.

The epoxy used for these experiments was Aeropoxy PR2032 resin with PH3660 curing agent. The Aeropoxy manufacturer, PTM&W, suggests a 100:27 wt/wt mixing ratio, cured at room temperature for 20 hours, followed by a 2-hour post cure at 80 °C. This polymer system has a 4 h pot life, providing ample time for degassing and processing. The mold is equipped with heating elements, allowing for the composites to be cured under pressure.

3.3.2 Wet Layup Manufacturing Method

Some rCF mats were also made into composites using a wet-layup process. During this process, a sheet of nylon is fixed to a flat metal plate. A layer of peel ply is then placed on the nylon, and layers of carbon fiber mat are placed over this peel ply. Epoxy was distributed across the surface of rCF Mats using a roller. Once enough fibers and epoxy were added, another layer of peel ply was placed on top of the fibers. A layer of porous nylon was placed over the peel ply, and a layer of breather was placed over the porous nylon. Another layer of non-porous nylon is placed over the layers, and sealed to the bottom layer of nylon. At this point, pressure is applied to the composite using a heated press, and a vacuum is pulled between the nylon layers. The epoxy is cured under vacuum at room temperature for 20 hours, followed by a 2-hour post-cure at 80 ℃ applied by the heated press. An example of composites manufactured using RTM and wet-layup are illustrated in Figure 28.

Figure 28 Examples of rCF composites manufactured using RTM (left) and wet-layup (right)

Chapter 4. Structural and Mechanical Characterization of Recycled Carbon Fiber Reinforced Polymer Composites (rCFRP)

4.1 Cross-sectional Microscopy

The cross-section of the tensile specimens was also examined. The fiber packing density and distribution of fibers within the composite can be observed in these cross-sectional images. These images were also used to verify the fiber volume fraction and alignment. Representative cross-sectional images are shown in Figure 29.

The microscopy samples were prepared by placing the composites into a silicon mold, which was filled with a two part fast-setting acrylic. Once cured, the sample was ground and polished with 120, 240, 400, 600, 1000, silicon carbide sandpaper and 6 micron and 1 micron diamond pastes. The samples were then cleaned with bath sonication in DI water, rinsed and dried with compressed air. The samples were imaged with an AmScope light microscope at 10x, 20x, and 40x.

The RTM micrographs show a very low presence of voids in the composite, along with relatively densely packed fibers. Most visible voids appear to be caused by removal of a few fibers during the grinding and polishing process. Overall, the fibers are well aligned, with a few highly misaligned fibers visible. Both of the wet-layup samples contained many large voids. These samples were all cured under vacuum. The reason for such high porosity has yet to be found. As expected, the non-aligned composite has many highly misaligned fibers. The wet layup samples appear

to have a lower fiber packing density, with the lowest fiber density apparent in the non-aligned sample.

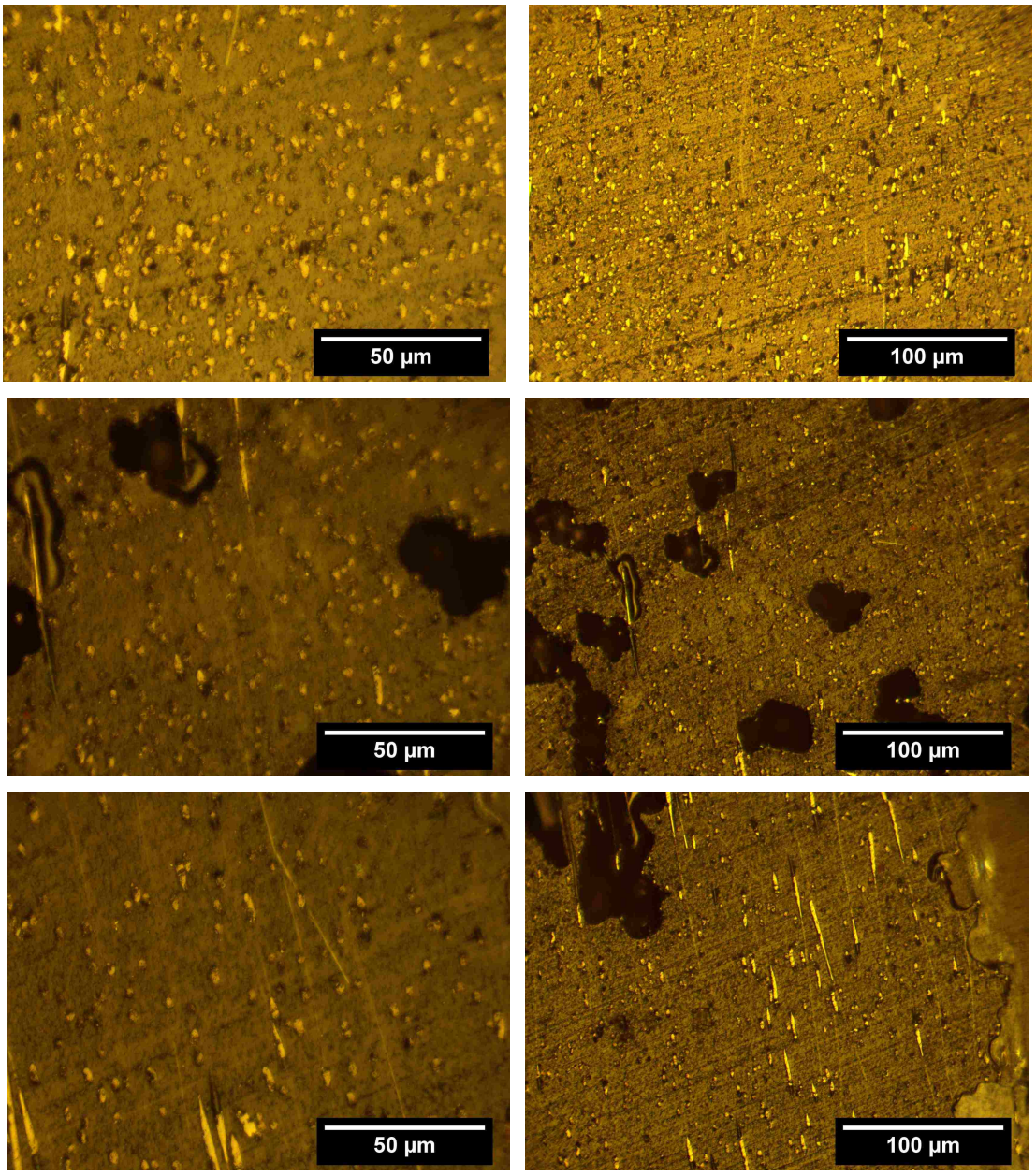

Figure 29 Micrographs of recycled carbon fiber composites. 10x (left) and 20x (right) magnification images are shown of an aligned, non-sized, RTM composite (top), an aligned, sized, wet-layup composite (middle), and a non-aligned, sized, wet-layup composite (bottom)

4.1.1 Void Content

The composite void content was found through analysis of the optical microscopy images. Each void was outlined by hand, and the total area of voids in each image was computed. This area was then compared to the total area of the corresponding image, and a void area percentage was calculated. 10x magnification images were used for this analysis, as they provide the largest area for analysis.

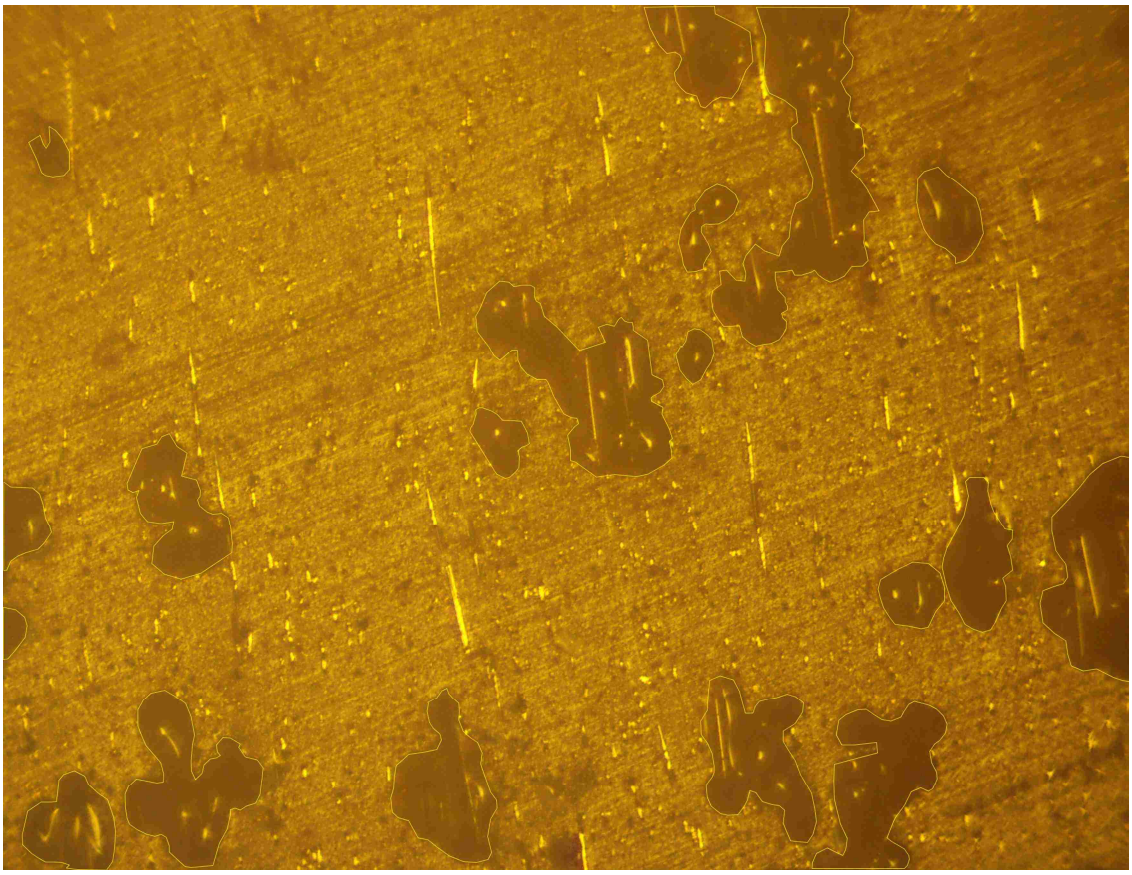

Figure 30 Void content analysis of wet-layup samples

Virtually no voids were observed for the RTM samples, which are therefore assumed to contain a void content of 0%. Images of the wet-layup samples containing outlined voids are shown in Figure 30. While the image covers a different area of the part, the void content was in close agreement for each image. The void content for the two wet-layup parts was found to be 15.66% and 15.82%, with an average of 15.74%

.

4.2 Volume Fraction Measurements

The volume fraction of the composites reported here were calculated by first weighing the fiber mats before manufacturing. After either wet-layup or RTM, the composite plates were measured with calipers. The volume of the composite was then calculated. The carbon fiber density was assumed to be 1.8 g/cc, which was used with the fiber mass to obtain a fiber volume. The fiber volume was then divided by the composite volume to achieve the composite fiber volume fraction. This method is expected to produce a fiber volume fraction near the actual volume fraction, though it is inherently error prone. For example, the composite plates, particularly for wet-layup, may not have uniform thickness after infusion. To account for this, many thickness measurements were taken around the perimeter of the part, and the average was used for the volume fracture calculation.

More precise volume fraction measurements were attempted using matrix digestion. The density was first measured using the Archimedes principal according to ASTM D792. For this measurement, the dry sample is first weighed in air. The buoyancy

force on the sample is then measured while the sample is submerged in DI water at 22 °C. The density of water is then used to calculate the volume of displaced liquid, which is equal to the volume of the submerged sample. Once the volume of the sample was known, ASTM D3171 was used to find the volume fraction of the sample using matrix digestion in nitric acid. The matrix digestion was attempted using 70% w/w nitric acid at 60 °C with stirring for 4 hours. However, the Aeropoxy used for these composites was found to resist digestion, and only a small quantity of the sample had dissolved after the 4 hours. The process was repeated, and the temperature of the solution was raised to 80 °C, and the sample was left submerged for 8 hours. Once removed from the solution, however, a sizable portion of the sample remained undissolved. Future research on this project will investigate alternative methods of obtaining a volume fraction of the recycled fiber composites manufactured with Aeropoxy to determine a precise volume fraction.

4.3 Micro Computed Tomography

4.4 Fractography

The fractured surface of the recycled carbon fiber composite was examined with various microscopic techniques. Firstly, the fracture surface of the tensile coupons was examined with a 12x macro-lens on a 12-megapixel camera (Figure 31). While this type of fracture was only observed on a few fractured surfaces, it indicates that stress in not effectively transferred between carbon fiber plies. The low interlaminar strength causes the plies to break at different regions rather than cleave in the same plane.

Figure 31 Fracture surface of carbon fiber composite specimen

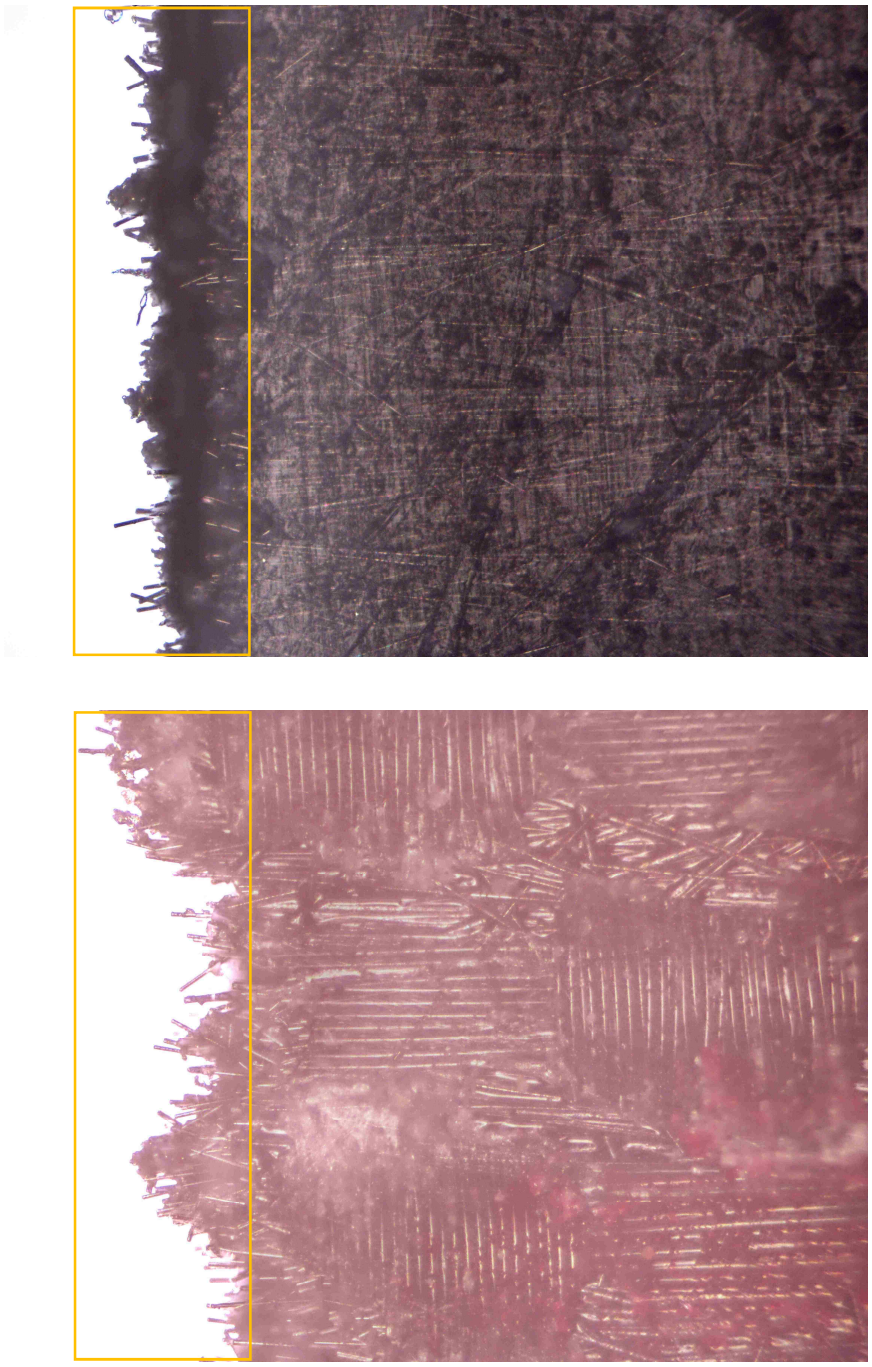

Figure 32 Micrograph of fractured surface of aligned, non-sized carbon fiber manufactured with RTM (top) and aligned, sized carbon fiber manufactured with wet-layup (bottom)

The micrographs shown in Figure 32 show that both sized and non-sized composites demonstrated fiber pull-out along the fracture surface. The significant amount of fiber pull-out is a direct result of weak interactions between the fibers and polymer. These images were taken at 20x magnification using extended depth of focus (EDF) on an AmScope microscope. EDF combines the highest contrast regions of multiple images captured at various distances from the objective, allowing for multiple areas of an image to appear in focus while they lie outside of a single focal plane. EDF image captures were also taken with the sample illuminated from above and below, which allow for viewing both the surface detail and high contrast pulled out fibers.

4.5 Tensile Tests

The tensile tests were used to determine the tensile strength and Young's modulus of the composite. A standard uniaxial tensile test applies either a fixed strain rate or load ramp to a material sample, and monitors the force on the sample with a load cell and strain on the sample with an extensometer. An example of the composite tensile test data is shown in Figure 33. The slope of the strain-strain curve in the elastic region is the Young's modulus, or modulus of elasticity, of the material. As carbon fibers are very brittle, there is essentially no yielding, or plastic deformation, of the material before fracture. The stress at which the part fractures is the strength of the material, and the strain at which it fractures is the strain to failure. The tensile test data in Figure 33 shows that the sample had a strength, stiffness, and strain to failure of approximately 200 MPa, 33.3 GPa, and 0.62%, respectively.

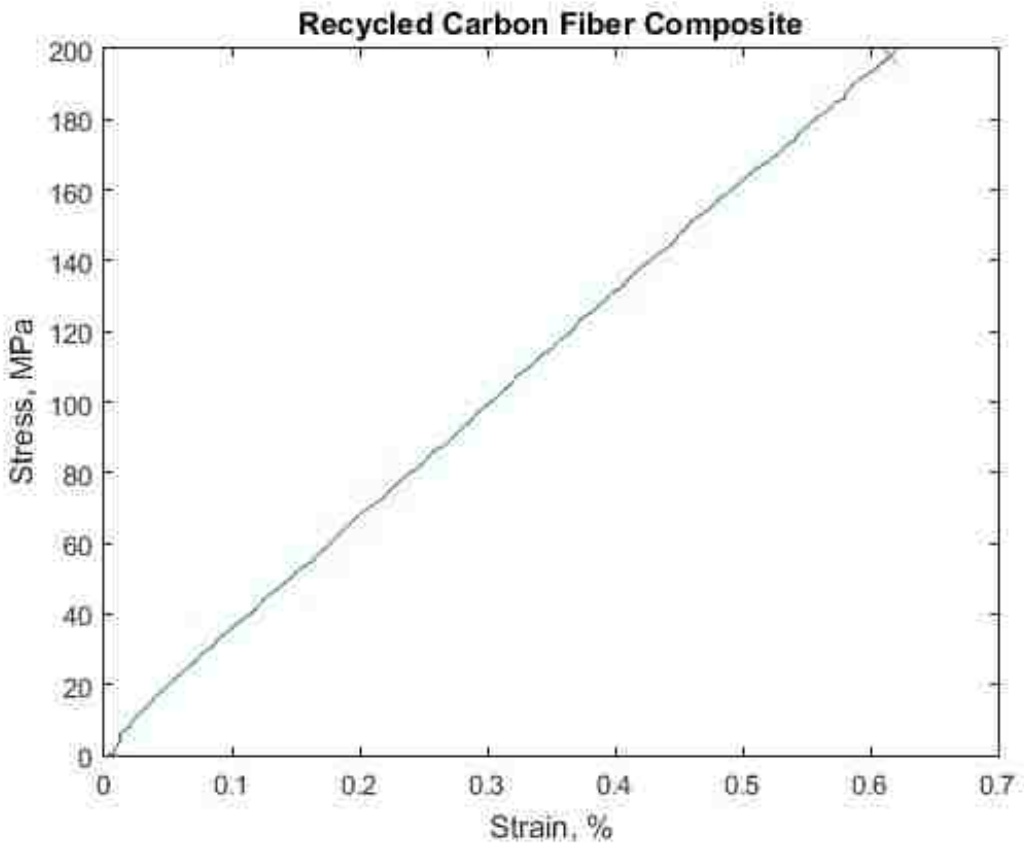

Figure 33. Tensile data for aligned, non-sized recycled carbon fiber composite.

The coupons for the tensile test were prepared following ASTM D3039/D3039M guidelines. The sample dimensions were approximately 1.0 x 15 x 127 mm. Fiberglass composite tabs, with dimensions of 25 x 1.3 mm and a 7° taper, were attached to each end, front and back, of the tensile coupons with Aeropoxy. The fiberglass tabs and ends of the carbon fiber composites were roughened with 240 grit silicon carbide paper to improve adhesion, and rinsed with acetone before epoxy was added. The epoxy was mixed and degassed, then used to adhere the tabs to the composite and fixed in place with clamps. The epoxy was allowed to cure for 20 hours, and subjected to a 2 hour post-cure at 80 ℃. These tabs are designed to minimize stress concentration between the coupon

and Instron clamps to prevent premature part failure. The tests were performed on an Instron 4400R, with a constant displacement rate of .05 in/min. Examples of the sample geometry and experimental setup are illustrated in Figure 34 and Figure 35, respectively.

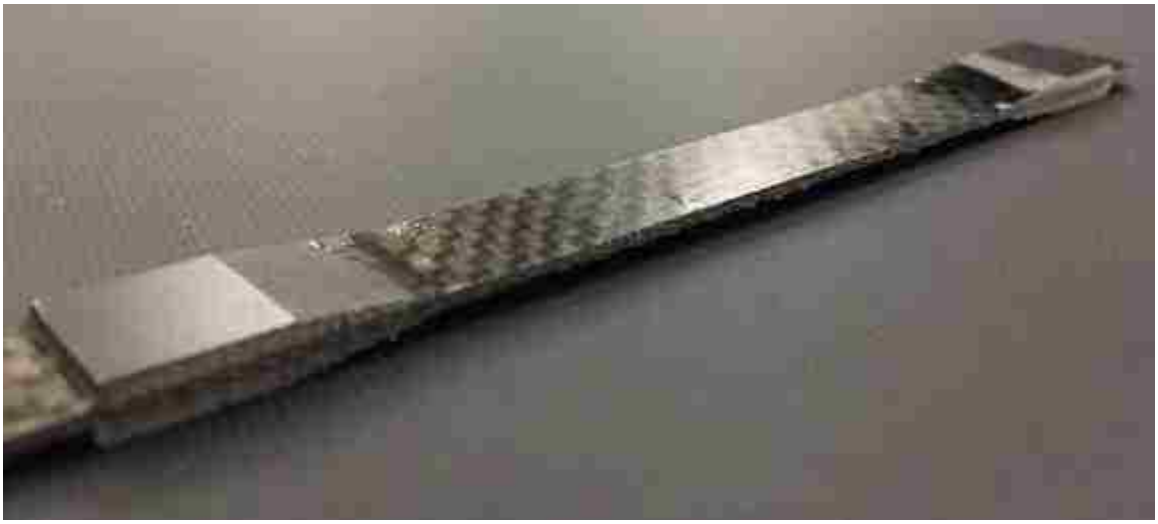

Figure 34 Example of tensile coupon and tab geometry.

Figure 35 Instron 4400R tensile test setup. The extensometer is attached with rectangular clips.

Tensile tests were performed on 5 coupons for each composite plate. The composites plates were made using sized, aligned fibers, non-sized, aligned fibers, sized, non-aligned fibers, and non-sized, non-aligned fibers. These plates were chosen to observe the differences in performance between sized and non-sized carbon fibers, and the effect of alignment on volume fraction and relative mechanical performance. The tensile strength and modulus data for these composites is given in Table 4.

Table 4. Strength and stiffness of recycled carbon fiber composites.

Sized	Aligned	V_f	Epoxy	Method	Strength (MPa)	Modulus (GPa)
Yes	Yes	24	Aeropoxy	Wet-layup	196	17.6
No	Yes	18	Aeropoxy	RTM	192	31.6
Yes	Yes	24	Aeropoxy	RTM	266	33.7
Yes	No	15	Aeropoxy	RTM	82.9	9.09

4.6 Discussions

It is now possible to correlate the fiber alignment, presence of sizing, and manufacturing method to the mechanical properties of the composite. We can analyze the effect of alignment by comparing the aligned, sized RTM samples with the non-aligned, sized RTM sample. In the case, the alignment results in an increase in the strength and modulus of the composite by 221% and 271%, respectively.

The effect of sizing can be found by comparing the aligned, sized RTM sample with the aligned, non-sized RTM sample. In this case, we observe an increase in the strength of the composite of 38.5%. However, the modulus is only increased by 6.68%. These results can be explained by the fact that all the carbon fiber in each composite contributes to the modulus, though the strength is heavily influence by the presence of aligned fibers. In general, the strength values are much lower than expected. This is most likely due to a low interfacial shear strength between the fiber and matrix. While XPS analysis show an activated rCF surface, the processing with water and glycerol has adversely affected the surfaces. We initially washed away the glycerol with warm water and subsequently evaporated the water at 180 °C. It seems like there was residual water

or glycerol on the carbon surface that inhibited carbon fiber bonding with epoxy during curing.

The effect of manufacturing method can be found by comparing the aligned, sized RTM composite with the aligned, sized wet-layup composite. The composite compared with wet-layup displayed a strength and modulus that were 35.78% and 91.53% higher than the wet-layup sample, respectively. The decrease in properties can largely be explained by the presence of voids in the samples prepared by wet layup, as seen in the cross-sectional micrographs (Figure 29). The fibers are not able to transfer the load effectively between each other due to the high void content, which results in the decrease in modulus of the composite. The strength, likewise, is heavily reduced as the voids also act as stress concentrators, which result in premature failure of the part.

Chapter 5. Theoretical Modeling of Strength and Stiffness in rCFRPs

5.1 Overview

Analytical models for prediction of tensile strength and stiffness of short fiber composite fibers have been developed and validated for discontinuous fiber composites.[46-50] In this chapter, we examine these models, for our recycled fiber composites, including the Halpin Tsai semi-empirical equations, composite mechanics approach and laminate analogy approach where we incorporate the experimentally measured fiber orientation and length distributions of the specimens.[46, 48] These analytical models will require exact description of fiber length/orientation distribution as well as fiber interfacial and tensile strength. All these values were experimentally calculated, as discussed in previous chapters. Theoretical modeling of the rCFRP will enable us to better understand the effects of fiber aspect ratio, alignment, volume fraction, and interfacial strength on composite properties and can guide design and re-manufacturing of rCFRP with enhanced mechanical properties.

5.2 Fiber Length and Orientation Distributions (FLD and FOD)

To predict the mechanical properties of discontinuous fiber composites distribution of fiber length and orientations should be properly defined. Both these can be mathematically described by probability density functions. The probability density function for fiber lengths or fiber length distribution (FLD) is defined such that the probability of fibers with length between l and $l+dl$ is $f(l)dl$. A similar probability

function, $g(\theta)$, can be defined for fiber orientation distribution (FOD). It is then obvious that:

$$\int_{l_{min}}^{l_{max}} f(x)dx = 1 \tag{4}$$

and,

$$\int_{\theta_{min}}^{\theta_{max}} g(\theta)d\theta = 1 \tag{5}$$

where l_{min} and l_{max} are the shortest and longest experimentally measured fiber lengths and θ_{min} and θ_{max} are the smallest and largest experimentally measured fiber angles, respectively. Experimental measurements of fiber length and orientation were sorted and stored in 'n' bins of equal width:

$$\Delta l = \frac{(l_{min} - l_{\max})}{n} \tag{6}$$

The population of the ith bin is represented with N_i. We can therefore write:

$$N = \sum_{i=1}^{n} N_i \tag{7}$$

$$f(l) = \frac{N_i/N}{\Delta l} \tag{8}$$

Similar equations can be used for FOD or $g(\theta)$. The experiential FLD and FOD can be then fitted to:

$$f(l) = abl^{b-1}\exp(-al^b) \tag{9}$$

for $l > 0$ and

$$g(\theta) = \frac{\sin\theta^{2p-1}\cos\theta^{2q-1}}{\int_{\theta_{min}}^{\theta_{max}} \sin\theta^{2p-1}\, cos\theta^{2q-1} d\theta} \tag{10}$$

for $0 \le \theta_{min} \le \theta \le \theta_{max} \le \pi/2$, where p and q are shape parameters that determine the FOD function shape. For example, if p=q=0.5, fibers are randomly distributed and for p=0.5 and q>100, almost all fibers are aligned in the 0° direction.

Experimental FLD and FOD were fit to equations (9) and (10) using the least square method in a Matlab script, as shown in Figure 36 and Figure 37. Fit parameters were found to be p=0.51, q=2.2, a=0.285, and b= 1.554.

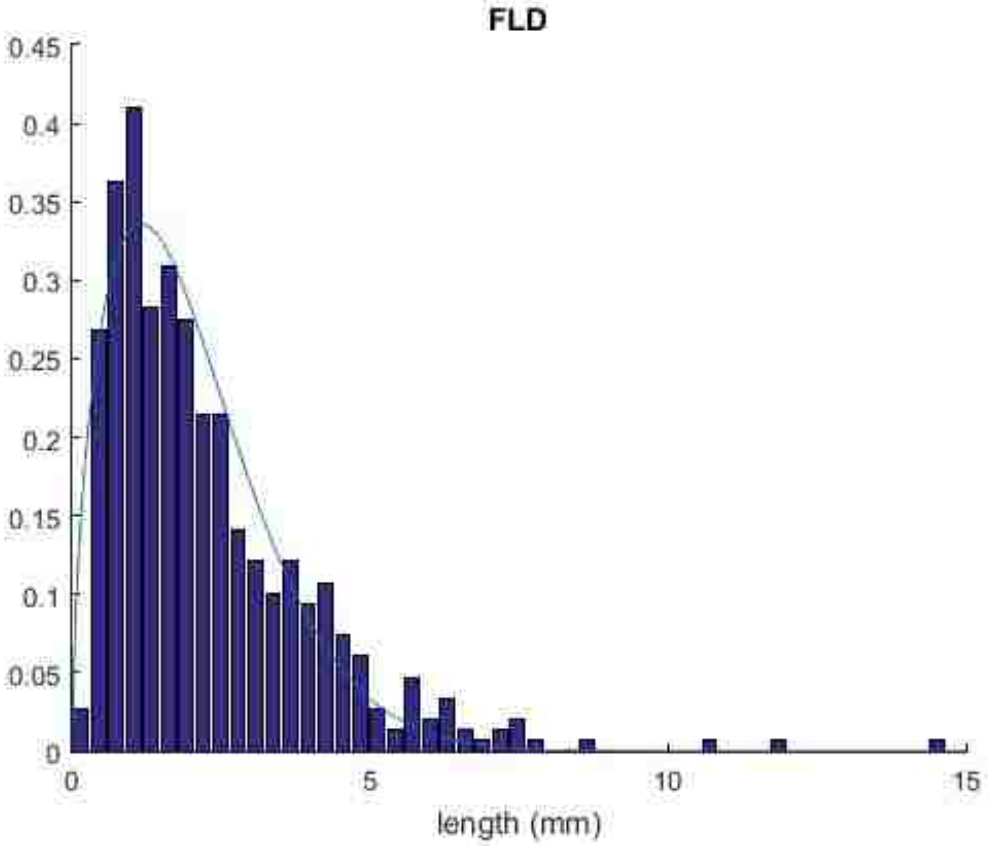

Figure 36 Recycled carbon fiber length distribution and curve fit (after processing)

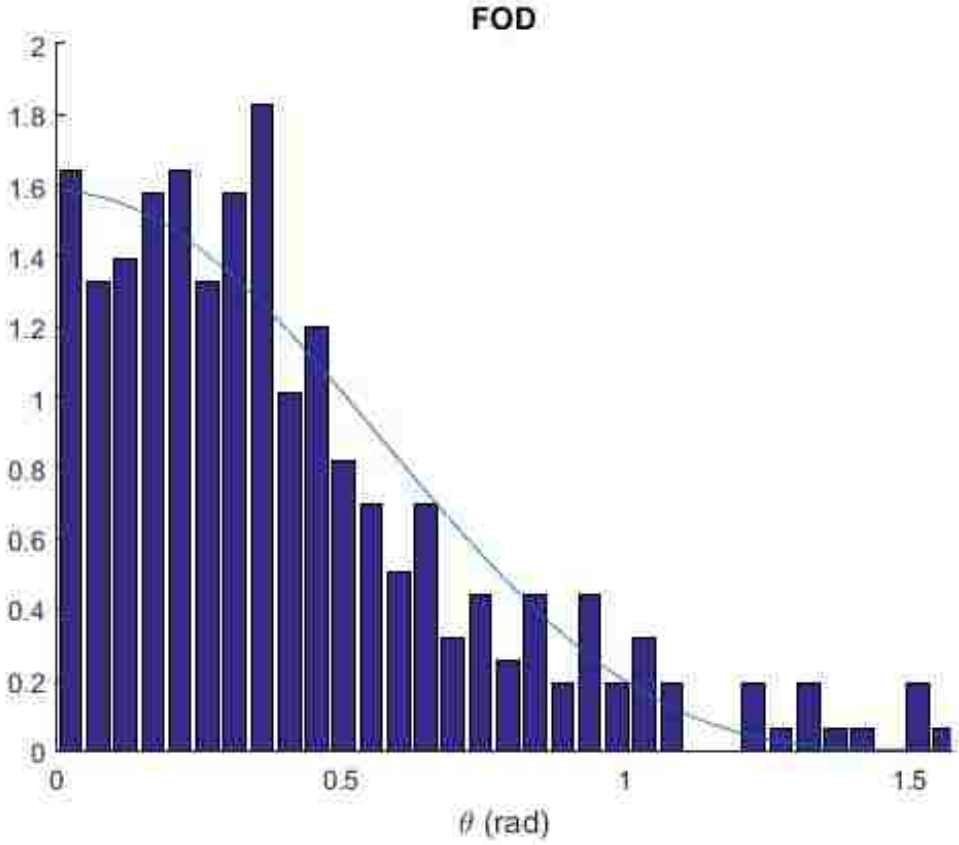

Figure 37 Fiber orientation distribution in rCF mats and curve fit

5.3 Tensile Strength of Partially Aligned Discontinuous Fiber Composites

Strength of partially aligned discontinues fiber composite can be estimated using mechanics approaches. In particular, when a load is exerted on a composite, interfacial shear stresses between fiber and matrix increase with increasing the applied load. Strength of the composite can be estimated by evaluating the average stress required to break the composite at some random cross section. Fiber failure in a composite depends strongly on the critical fiber length. For a single fiber that intersects a crack at an angle, θ:

$$\sigma_{F\theta}^{\mu} = \sigma_F^{\mu}\left[1 - A_f \tan(\theta)\right] \tag{11}$$

where A_f is a constant and equals 0.083 for a carbon-epoxy system and σ_F is the strength of fiber when the crack plan is perpendicular to fiber axis [50]. The critical length of an oblique fiber can be written as:

$$l_{c\theta} = \frac{l_c\left[1 - A_f \tan(\theta)\right]}{\exp(\mu\theta)} \tag{12}$$

where μ is the snubbing friction and is estimated as 0.1 in our model [51].

Strength of composite can be calculated using the following expression:

$$\sigma_c^{\mu} = \chi_1\chi_2\sigma_F^{\mu}\nu + \sigma_M\nu_m \tag{13}$$

$$\chi_1\chi_2 = \int_{\theta_{min}}^{\theta_{max}} \int_{l_{min}}^{l_{c\theta}} f(l)g(\theta)(l\backslash l_{mean})(l\backslash 2l_C))\exp(\mu\theta)\mathrm{d}/\mathrm{d}\theta \tag{14}$$

$$+ \int_{\theta_{min}}^{\theta_{max}} \int_{l_{c\theta}}^{l_{max}} f(l)g(\theta)(l\backslash l_{mean})(1 - A_f \tan(\theta))$$

$$\times (1 - l_c(1 - A_f \tan(\theta))/(2l \exp(\mu\theta)))d/d\theta$$

χ_1 and χ_2 are fiber orientation factor and fiber length factor, respectively. For example, for a composite with perfectly aligned fibers of different length χ_1 is 1, and if fibers are infinitely long, χ_2 is 1.

5.4 Tensile Modulus of Partially Aligned Discontinuous Fiber Composites

Elastic moduli of discontinuous fiber composites can be calculated using the laminate analogy approach where short fibers are simulated as sequential stacks of various laminae with different orientation and fiber lengths. Elastic stresses-strain relationship, assuming a plane stress, in a composite laminate in the 0° orientation is written as:

$$\begin{Bmatrix} \sigma_1 \\ \sigma_2 \\ \tau_{12} \end{Bmatrix} = \begin{Bmatrix} Q_{11} & Q_{12} & Q_{16} \\ Q_{12} & Q_{22} & Q_{26} \\ Q_{16} & Q_{26} & Q_{66} \end{Bmatrix} \begin{Bmatrix} \varepsilon_1 \\ \varepsilon_2 \\ \gamma_{12} \end{Bmatrix} \tag{15}$$

where

$$Q_{11} = \frac{E_{11}}{1 - \nu_{12}\nu_{21}} \tag{16}$$

$$Q_{12} = \nu_{21}Q_{11} \tag{17}$$

$$Q_{16} = 0 \tag{18}$$

$$Q_{22} = \frac{E_{22}}{1 - \nu_{12}\nu_{21}} \tag{19}$$

$$Q_{26} = 0 \tag{20}$$

$$Q_{66} = G_{12} \tag{21}$$

For a laminate that is off-axis stress-strain relation is:

$$\begin{Bmatrix} \sigma_1' \\ \sigma_2' \\ \tau_{12}' \end{Bmatrix} = \begin{Bmatrix} Q_{11}' & Q_{12}' & Q_{16}' \\ Q_{12}' & Q_{22}' & Q_{26}' \\ Q_{16}' & Q_{26}' & Q_{66}' \end{Bmatrix} \begin{Bmatrix} \varepsilon_1' \\ \varepsilon_2' \\ \gamma_{12}' \end{Bmatrix} \tag{22}$$

where the Q' matrix is calculated as:

$$\begin{Bmatrix} Q_{11}' \\ Q_{22}' \\ Q_{12}' \\ Q_{66}' \\ Q_{16}' \\ Q_{26}' \end{Bmatrix} = \begin{Bmatrix} m^4 & n^4 & 2m^2n^2 & 4m^2n^2 \\ n^4 & m^4 & 2m^2n^2 & 4m^2n^2 \\ m^2n^2 & m^2n^2 & m^4 + n^4 & -4m^2n^2 \\ m^2n^2 & m^2n^2 & -2m^2n^2 & (m^2 - n^2)^2 \\ m^3n & -mn^3 & mn^3 - m^3n & 2(mn^3 - m^3n) \\ mn^3 & -m^3n & m^3n - mn^3 & 2(m^3n - mn^3) \end{Bmatrix} \begin{Bmatrix} Q_{11} \\ Q_{22} \\ Q_{12} \\ Q_{66} \end{Bmatrix} \tag{23}$$

where m=cosθ and n=sinθ. The laminate stiffness matrix for the discontinuous fiber composite is then calculated as:

$$\bar{A}_{ij} = \int_{l_{min}}^{l_{max}} \int_{\theta_{min}}^{\theta_{max}} \frac{Q_{ij}' f(l) g(\theta) d}{d\theta} \tag{24}$$

and finally, the composite tensile modulus is calculated using:

$$\bar{E}_{11} = \frac{\bar{A}_{11}\bar{A}_{22} - \bar{A}_{12}^2}{\bar{A}_{22}} \tag{25}$$

Elastic constants for unidirectional fiber composites were estimated from the Hapin-Tsai equations,[52] as follows:

$$E_c = E_{11} = \frac{1 + 2\eta_L \nu}{1 - \eta_L \nu} E_m \tag{26}$$

$$\nu_{12} = \nu_f \nu + \nu_m \nu_m \tag{27}$$

$$\nu_{21} = \frac{E_{22}}{E11} \nu_{12} \tag{28}$$

$$G_{12} = \frac{1 + \eta_g \nu}{1 - \eta_g \nu} G_m \tag{29}$$

where

$$\eta_L = \frac{\frac{E_f}{E_m} - 1}{\frac{E_f}{E_m} + 2\left(\frac{l}{d}\right)} \tag{30}$$

$$\eta_T = \frac{\frac{E_f}{E_m} - 1}{\frac{E_f}{E_m} + 2} \tag{31}$$

$$\eta_G = \frac{\frac{G_f}{G_m} - 1}{\frac{G_f}{G_m} + 1} \tag{32}$$

Finally, the fiber orientation coefficient, f_θ, was used to describe the average orientation of fibers in the mat, where f_θ varies between -1 and 1, with -1 corresponding to fibers that are perpendicular to the measurement direction, 0 for random fiber orientation, and 1 corresponding to uni-axially aligned fibers:

$$f_\theta = \int_{\theta_{min}}^{\theta_{max}} g(\theta)\cos^2(\theta)\,d\theta - 1 \tag{33}$$

5.5 Results and Discussions

The relationship between the normalized composite modulus and fiber orientation angle is plotted in Figure 38; modulus values were normalized to the modulus of a composite with infinitely long fibers and a 20% volume fraction. A volume fraction of 20%, similar to the experimentally tested samples, was used for this model. It should be noted that the fiber critical length does not affect the modulus. As expected, as the fibers become more aligned along the tensile axis, the composite modulus monotonically

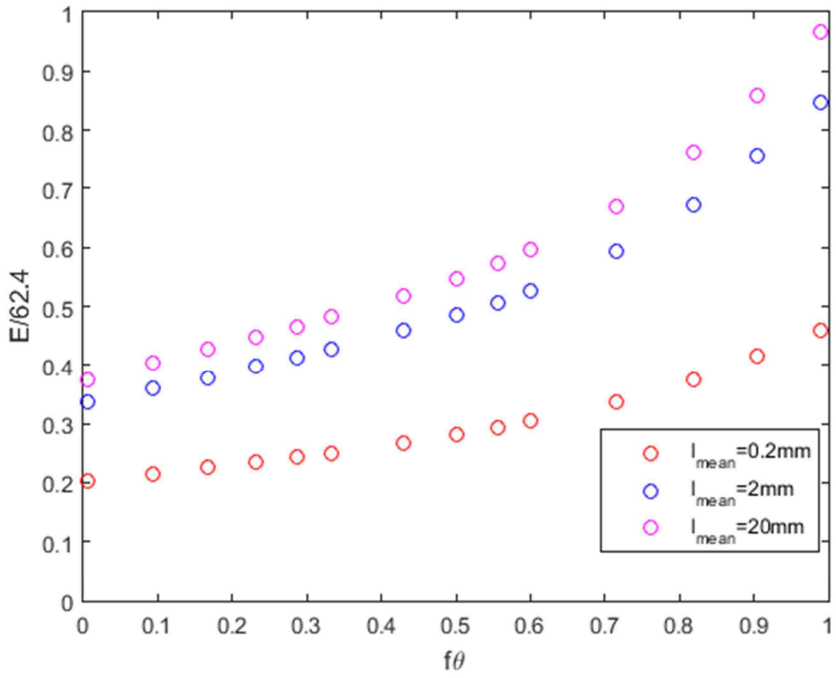

Figure 38 Normalized modulus as a function of fiber alignment. $f\theta = 0$ corresponds to randomly oriented fibers, while $f\theta = 1$ corresponds to perfectly aligned fibers.

increases. While this trend is also apparent for different mean fiber lengths, it is more dramatic for larger fiber lengths. For example, the difference in normalized modulus for aligned and randomly oriented fibers with a mean length of 0.2mm is roughly 2.5, while the same difference for a mean fiber length of 2mm is 4. Additionally, the trend observed in this plot is not linear, which illustrates the importance of increasing the fiber orientation above an f_θ of 0.7. Therefore, it can be concluded that through maintaining a minimum mean fiber length of 2mm while achieving an f_θ of greater than 0.7 will be required for producing high modulus composites.

The relationship between normalized modulus and mean fiber length is investigated in Figure 39. Again, the intuitive trend of increasing modulus with increasing mean fiber length is observed, However, this plot demonstrates the importance

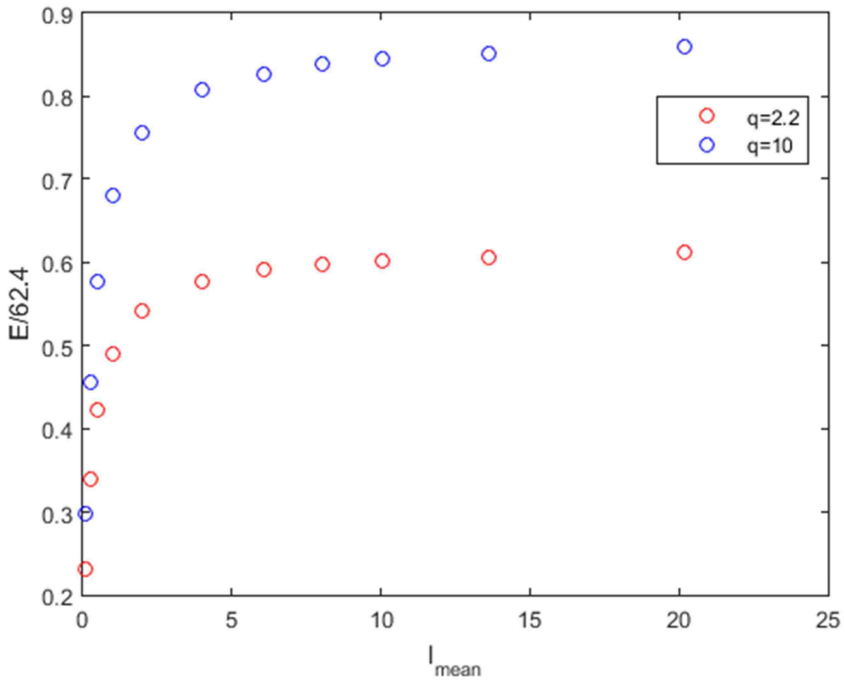

Figure 39 Normalized modulus as a function of mean fiber length (mm). q=2.2 corresponds to weakly aligned fibers, while q=10 corresponds to strongly aligned fibers.

of maintaining a mean fiber length on the millimeter scale. For both weakly and strongly aligned fibers, the normalized modulus is dramatically reduced below 5mm mean lengths. Increasing the mean fiber length above 5mm does not produce a significant increase in the composite modulus. Therefore, it appears necessary to maintain a mean fiber length of 5mm to produce composites with a competitive modulus.

The parameter χ_{12} can be used to predict the composite strength, where it varies between 0 and 1, with 1 representing the maximum composite strength. The relationship between χ_{12} and f_θ is illustrated in Figure 40. For a long critical fiber length (4mm), there does not appear to be a dependence of composite strength on fiber orientation. However, at low critical lengths (0.25mm), fiber alignment does increase the strength of the composite. However, the increase in strength is diminished above an $f\theta$ of 0.5, above

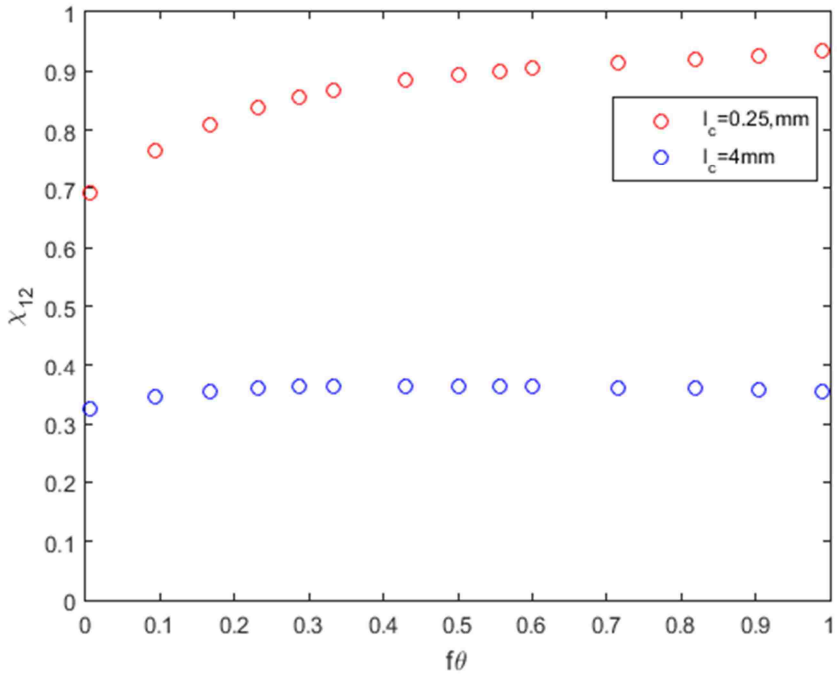

Figure 40 χ_{12} as a function of fiber orientation for two given critical lengths.

which the composite can be expected to achieve a strength near the optimum value. It can be concluded that the fiber critical length determines the strength of composites while fiber orientation has a lower influence on the strength. This is contrary to the modulus dependence on orientation where there exists a strong relationship.

The dependence of strength on mean fiber length was also explored. For a low critical fiber length (0.25mm), the strength reaches a plateau at a fiber length of only a few millimeters. Above 5mm, only slight improvements to strength are observed for an increase in mean fiber length. At higher critical fiber lengths, however, increasing the mean fiber length continues to produce improvements in strength up to centimeter scale mean fiber lengths. This indicates that strength can be maximized at low mean fiber

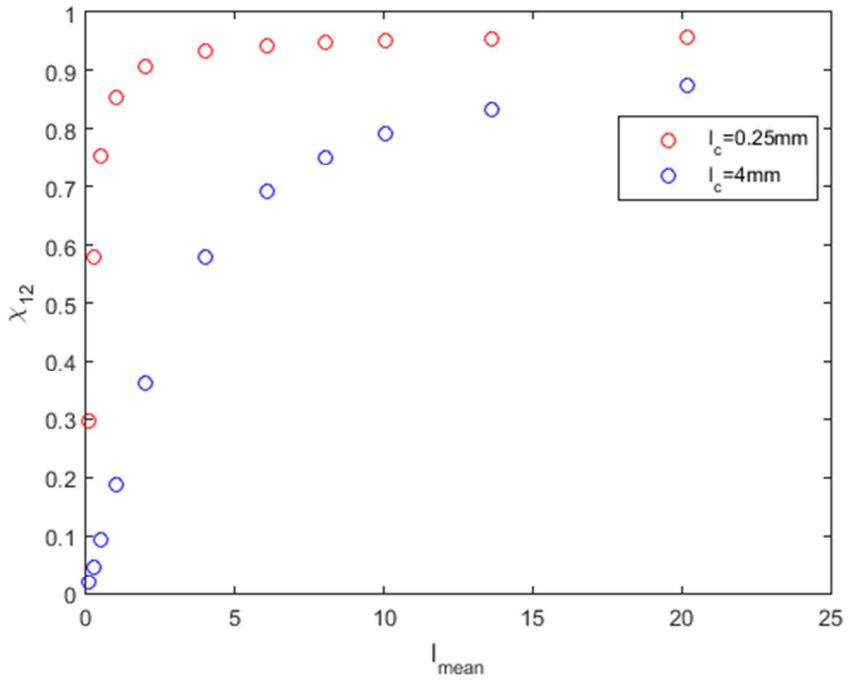

Figure 41 χ_{12} as a function of mean fiber length (mm) for two given critical lengths.

lengths when the critical length is small, while long fibers are necessary to increase strength for longer critical lengths.

In summary, an f_θ and l_{mean} above 0.7 and 5mm, respectively, can be expected to produce a high modulus composite. Similarly, a mean fiber length above 3mm is expected to produce a high strength composite for short critical lengths, while a mean fiber length above 10mm is required for longer critical lengths.

The volume faction has a nearly linear relationship with both strength and modulus values in composites. Volume fraction can be increased if the compression pressure during manufacturing is high enough to cause fibers to cut each other, into shorter length, and therefore a higher packing is achieved. It is therefore critical to optimize the FLD, FOD and volume fraction for rCFRPs. Solving this problem numerically or analytically proved to be an extremely challenging task and we therefore plan to perform experiments to find the interrelationships between FOD, FLD and maximum packing fraction. This will in turn allow us to optimize the processing parameters to achieve desired combinations of stiffness and strength.

Chapter 6. Conclusions and Future Work

6.1 Summary of Results

The effect of alignment, sizing, and manufacturing method of recycled carbon fiber composites was investigated experimentally and theoretically. Randomly oriented 2D carbon fiber mats were manufactured through a dispersion and filtration method. Aligned carbon fiber mats were manufactured using a similar dispersion process coupled with a centrifugal alignment rig. A selection of fibers was taken without further processing after recycling, which were found to exhibit a relatively low surface activation. Therefore, a sizing agent was applied to a portion of these fiber with the intention of improving the interfacial shear strength between the fiber surface and epoxy matrix. The composites were manufactured using either wet-layup or resin transfer molding (RTM).

The degree of fiber alignment in the remanufactured RCF mats was characterized using the FibrilTool plugin with ImageJ on microscopy images. It was found that, on highly aligned composites, roughly 70% of fibers were aligned within 15° of the mean direction. The results from FibrilTool were used to characterize 128 micrographs of aligned fibers to determine the optimal mode of three processing parameters in a two-factorial experiment. The effect of processing on the average fiber length and surface activation was also evaluated. The average length was found to be roughly 1.5 mm, which was still well above the critical fiber length.

The presence and effect of sizing was evaluated using SEM, XPS, and single fiber fragmentation tests. Analysis of SEM micrographs did not show any substantial

degradation or additional particulates on the fiber surface after the sizing process. XPS did show an increase in active chemical groups on the fiber surface, which are known to bond with the epoxy used in this study. Additionally, the sized fibers displayed an increase in interfacial shear strength (IFSS) over non-sized fibers, though the IFSS was not as high as that of virgin fiber.

To determine the precise influence of each variable, four recycled fiber composites were manufactured. The effect of sizing was found by comparing two aligned, RTM composites prepared with either sized or non-sized fibers. The influence of alignment was found by comparing two sized, RTM composites, manufactured using either aligned or non-aligned rCF mats. Lastly, the effect of manufacturing process was found by comparing two composites made with sized, aligned fibers manufactured using either RTM or wet-layup.

The degree of alignment was unsurprisingly found to have the largest influence on the strength and stiffness of the composites. Both sized, randomly oriented 2D mats and aligned mats were infused using RTM. The aligned composite was found to have an increase in strength and stiffness of 221% and 271%, respectively, over the non-aligned composite. In general, transverse fibers are known to contribute very little to the strength or stiffness of carbon fiber composites. The aligned, sized RTM mat displayed the highest properties of those tested, while the non-aligned, sized mat was found to have the lowest properties. It can be concluded that highly aligned fiber mats are necessary to produce competitive parts with recycled carbon fibers.

While sizing has little influence on the elastic modulus of the composites (6.7% increase), there was a more substantial increase in the composite strength (38.5%). It can

be concluded that, in general, the interfacial shear strength of a composite filler will significantly affect the strength of a composite with a relatively low change in modulus. At relatively low stresses, the fiber fillers all contribute to the elastic elongation of the material regardless of interfacial shear strength (within these bounds). However, at stresses near the strength of the composite the fibers do not effectively transfer stresses between one another, begin to fail at the fiber edges/interfaces, or some combination of these mechanisms.

Lastly, the influence of manufacturing method was found by comparing aligned, sized fiber composites infused using either RTM or wet-layup. In this case, RTM displayed superior strength and stiffness over wet-layup composites, with a strength and stiffness increase of 35.78% and 91.53%, respectively. The wet-layup micrographs displayed a relatively high void content, which is likely responsible for the decrease in composite properties. The reason for the observed porosity in this part in uncertain, as the epoxy was allowed ample time to degas under vacuum. It is possible that the addition of pressure while the epoxy was degassing entrapped the gasses between fibers, or possibly that the vacuum was not sufficiently strong to remove the gas from the epoxy. The voids act as stress concentrators within the composite, which reduces the strength of the part. The fibers are not available to transfer stress within the voids, which likely is responsible for the reduction in modulus.

At this point, it may be useful to compare the material properties obtained here to those of common low-density materials used in various industries. Aluminum 6061-T6 is a popular aluminum alloy against which a low-cost carbon fiber composite may have an edge. The strength and stiffness of aluminum 6061-T6 is 310 MPa and 68.9 GPa,

respectively, while the aligned, sized, RTM manufactured recycled carbon fiber composite presented here has a strength and stiffness of 266 MPa and 33.7 GPa, respectively. However, the density of the carbon fiber composite is roughly 1.32 g/cc, while that of the aluminum allow is 2.7 g/cc. This give a specific strength and stiffness of 114.9 MPa/g/cc and 25.5 GPa/g/cc, respectively, for aluminum T6061-T6, and 205.51 MPa/g/cc and 25.53 GPa/g/cc, respectively, for the recycled fiber composite. Given these properties, it appears feasible that with improvements to the alignment and manufacturing process, the low cost of recycled carbon fiber may one day produce competitive composites for high strength, high stiffness, and low-density applications.

The model used in this study indicated that low fiber lengths could dramatically reduce the strength and modulus of the composites. This result suggests that further effort may be needed to maintain longer fibers during the dispersion and alignment process. Ideally, fibers over 5mm in length can be expected to produce composites with exceptional strength and modulus, though the average fiber length in this study was close to 2mm. Additionally, a low critical length is necessary to improve the strength of the composites. Further work is necessary to quantify the critical length of fibers in this study, and possibly investigate alternative sizing or surface activation methods to improve interfacial shear strength. Lastly, improving fiber alignment can be expected to increase the composite modulus, though the strength is likely to only experience marginal improvements. This model provides valuable insight into the appropriate parameters to target to produce the highest strength and modulus rCFRPs in future studies.

6.2 Sources of Error

The first primary source of error is a low sample size. Due to the time intensive process of processing and manufacturing each composite, particularly for aligned fiber composites, only a single composite plate was made for each sample. While 5 or more samples were retrieved and tested from each composite, this does not speak to the reproducibility of each method. Small variations in processing conditions, epoxy mixing ratios, ambient humidity and temperature, exact time of degassing before infusion, and total pressure applied to the mold may exist for each composite, and the effect of those variations is unknown. In general, great care was taken to ensure all the processing and manufacturing conditions were identical, but the robustness of the system with respect to each parameter has not been characterized.

Additionally, contaminates were observed in the composite with micro-computed tomography (not shown here). There were very little contaminates observed with SEM or light microscopy, though the sample size for SEM was very small and light microscopy may not have displayed sufficient contrast between fibers and contaminates. The composition and overall prevalence of these particles has not been determined. However, it is likely that they are much weaker than carbon fiber and may not bond strongly with the epoxy, and therefore may act only as volume defects within the polymer matrix.

The use of light microscopy for the alignment characterization was also problematic. In general, only a selection of fiber would fall within the focal plane for each image. While compressing these fibers between glass slides increased the number of fibers that could be captured in focus within each image, consistent portions of the image would not be in focus. This likely diminished the consistency of FibrilTool in computing

the anisotropy score of each image. This also accounts for the difference in anisotropy score for processed and non-processed images, as out of portions of the image would manifest differently in the image after processing.

6.3 Future Work

There is still a substantial need for research to improve the scalability of effectiveness of carbon fiber alignment techniques. A low-cost, scalable, and highly effective method of discontinuous fiber alignment would be a disruptive technology capable of bringing recycled carbon fiber composites into high-volume markets. It has been demonstrated here that even at relatively low volume fractions, aligned recycled carbon fiber composites can compete with commonly used industrial materials. At only $1/10^{th}$ the cost of virgin carbon fiber and comparable mechanical properties, there remains enormous room for growth in the incorporation of recycled carbon fibers into high volume markets.

References

1. Holmes, M., Global carbon fibre market remains on upward trend. *Reinforced Plastics* **2014,** *58* (6), 38-45.

2. Campbell, F. C., *Structural composite materials*. ASM international: **2010**.

3. Wood, K., Carbon fiber reclamation: going commercial. *High Performance Composites* **2010,** *3*, p1-2.

4. Witik, R. A.; Teuscher, R.; Michaud, V.; Ludwig, C.; Manson, J. A. E., Carbon fibre reinforced composite waste: An environmental assessment of recycling, energy recovery and landfilling. *Compos Part a-Appl S* **2013,** *49*, 89-99.

5. Pimenta, S.; Pinho, S. T., Recycling carbon fibre reinforced polymers for structural applications: Technology review and market outlook. *Waste Manage* **2011,** *31* (2), 378-392.

6. Schinner, G.; Brandt, J.; Richter, H., Recycling carbon-fiber-reinforced thermoplastic composites. *J Thermoplast Compos* **1996,** *9* (3), 239-245.

7. Yip, H. L. H.; Pickering, S. J.; Rudd, C. D., Characterisation of carbon fibres recycled from scrap composites using fluidised bed process. *Plast Rubber Compos* **2002,** *31* (6), 278-282.

8. Pickering, S. J., Recycling technologies for thermoset composite materials - current status. *Compos Part a-Appl S* **2006,** *37* (8), 1206-1215.

9. Pinero-Hernanz, R.; Dodds, C.; Hyde, J.; Garcia-Serna, J.; Poliakoff, M.; Lester, E.; Cocero, M. J.; Kingman, S.; Pickering, S.; Wong, K. H., Chemical recycling of carbon fibre reinforced composites in nearcritical and supercritical water. *Compos Part a-Appl S* **2008,** *39* (3), 454-461.

10. Jiang, G.; Pickering, S. J.; Lester, E. H.; Turner, T. A.; Wong, K. H.; Warrior, N. A., Characterisation of carbon fibres recycled from carbon fibre/epoxy resin composites using supercritical n-propanol. *Compos Sci Technol* **2009,** *69* (2), 192-198.

11. Liu, Y. Y.; Shan, G. H.; Meng, L. H., Recycling of carbon fibre reinforced composites using water in subcritical conditions. *Mat Sci Eng a-Struct* **2009,** *520* (1-2), 179-183.

12. Nahil, M. A.; Williams, P. T., Recycling of carbon fibre reinforced polymeric waste for the production of activated carbon fibres. *J Anal Appl Pyrol* **2011,** *91* (1), 67-75.

13. Jiang, G. Z.; Pickering, S. J., Recycled carbon fibres: contact angles and interfacial bonding with thermoset resins. *Mater Sci Forum* **2012,** *714*, 255-261.

14. Knight, C. C.; Zeng, C. C.; Zhang, C.; Wang, B., Recycling of woven carbon-fibre-reinforced polymer composites using supercritical water. *Environ Technol* **2012,** *33* (6), 639-644.

15. Meredith, J.; Cozien-Cazuc, S.; Collings, E.; Carter, S.; Alsop, S.; Lever, J.; Coles, S. R.; Wood, B. M.; Kirwan, K., Recycled carbon fibre for high performance energy absorption. *Compos Sci Technol* **2012,** *72* (6), 688-695.

16. Morin, C.; Loppinet-Serani, A.; Cansell, F.; Aymonier, C., Near- and supercritical solvolysis of carbon fibre reinforced polymers (CFRPs) for recycling carbon fibers as a valuable resource: State of the art. *J Supercrit Fluid* **2012,** *66*, 232-240.

17. Wang, Y. Q.; Cui, X. J.; Ge, H.; Yang, Y. X.; Wang, Y. X.; Zhang, C.; Li, J. J.; Deng, T. S.; Qin, Z. F.; Hou, X. L., Chemical Recycling of Carbon Fiber Reinforced Epoxy Resin Composites via Selective Cleavage of the Carbon-Nitrogen Bond. *Acs Sustain Chem Eng* **2015,** *3* (12), 3332-3337.

18. Yang, J.; Liu, J.; Liu, W. B.; Wang, J.; Tang, T., Recycling of carbon fibre reinforced epoxy resin composites under various oxygen concentrations in nitrogen-oxygen atmosphere. *J Anal Appl Pyrol* **2015,** *112*, 253-261.

19. Jiang, G. Z.; Pickering, S. J., Structure-property relationship of recycled carbon fibres revealed by pyrolysis recycling process. *J Mater Sci* **2016,** *51* (4), 1949-1958.

20. Matthew Such, C. W., Kevin Potter, Aligned Discontinuous Fibre Composites: A Short History. *Journal of Multifunctional Composites* **2014,** *3*, 155-168.

21. McNally, T.; Boyd, P.; McClory, C.; Bien, D.; Moore, I.; Millar, B., Recycled carbon fiber filled polyethylene composites. *J Appl Polym Sci* **2008,** *107* (3), 2015-2021.

22. Turner, T. A.; Warrior, N. A.; Pickering, S. J., Development of high value moulding compounds from recycled carbon fibres. *Plast Rubber Compos* **2010,** *39* (3-5), 151-156.

23. Wong, K. H.; Pickering, S. J.; Rudd, C. D., Recycled carbon fibre reinforced polymer composite for electromagnetic interference shielding. *Compos Part a-Appl S* **2010,** *41* (6), 693-702.

24. Pimenta, S.; Pinho, S. T.; Robinson, P.; Wong, K. H.; Pickering, S. J., Mechanical analysis and toughening mechanisms of a multiphase recycled CFRP. *Compos Sci Technol* **2010,** *70* (12), 1713-1725.

25. Turner, T. A.; Pickering, S. J.; Warrior, N. A., Development of recycled carbon fibre moulding compounds - Preparation of waste composites. *Compos Part B-Eng* **2011,** *42* (3), 517-525.

26. Pinho, S. T.; Gutkin, R.; Pimenta, S.; De Carvalho, N. V.; Robinson, P., On longitudinal compressive failure of carbon-fibre-reinforced polymer: from unidirectional to woven, and from virgin to recycled. *Philos T R Soc A* **2012,** *370* (1965), 1871-1895.

27. Wong, K. H.; Mohammed, D. S.; Pickering, S. J.; Brooks, R., Effect of coupling agents on reinforcing potential of recycled carbon fibre for polypropylene composite. *Compos Sci Technol* **2012,** *72* (7), 835-844.

28. Feng, N.; Wang, X. D.; Wu, D. Z., Surface modification of recycled carbon fiber and its reinforcement effect on nylon 6 composites: Mechanical properties, morphology and crystallization behaviors. *Curr Appl Phys* **2013,** *13* (9), 2038-2050.

29. Okajima, I.; Hiramatsu, M.; Shimamura, Y.; Awaya, T.; Sako, T., Chemical recycling of carbon fiber reinforced plastic using supercritical methanol. *J Supercrit Fluid* **2014,** *91*, 68-76.

30. Pimenta, S.; Pinho, S. T., The influence of micromechanical properties and reinforcement architecture on the mechanical response of recycled composites. *Compos Part a-Appl S* **2014,** *56*, 213-225.

31. Yu, H.; Potter, K. D.; Wisnom, M. R., A novel manufacturing method for aligned discontinuous fibre composites (High Performance-Discontinuous Fibre method). *Compos Part a-Appl S* **2014,** *65*, 175-185.

32. Gosau, J.-M.; Wesley, T. F.; Allred, R. E. In *Integrated composite recycling process*, Proceedings of the 38th SAMPE technical conference, **2006**.

33. Allred, R. E.; Haight, A. E. H.; Wesson, S. P., Effect of Reactive Finishes on the Moisture Durability of Carbon/Vinyl Ester Laminates. **2010**.

34. Johnson, D. J., Structure Property Relationships in Carbon-Fibers. *J Phys D Appl Phys* **1987,** *20* (3), 286-291.

35. Tang, L. G.; Kardos, J. L., A review of methods for improving the interfacial adhesion between carbon fiber and polymer matrix. *Polym Composite* **1997,** *18* (1), 100-113.

36. Dai, Z. S.; Shi, F. H.; Zhang, B. Y.; Li, M.; Zhang, Z. G., Effect of sizing on carbon fiber surface properties and fibers/epoxy interfacial adhesion. *Appl Surf Sci* **2011,** *257* (15), 6980-6985.

37. Weitzsacker, C. L.; Xie, M.; Drzal, L. T., Using XPS to investigate fiber matrix chemical interactions in carbon-fiber-reinforced composites. *Surf Interface Anal* **1997,** *25* (2), 53-63.

38. Feih, S.; Wonsyld, K.; Minzari, D.; Westermann, P.; Lilholt, H. *Testing procedure for the single fiber fragmentation test*; Forskningscenter Risø: **2004**.

39. Sager, R. J.; Klein, P. J.; Lagoudas, D. C.; Zhang, Q.; Liu, J.; Dai, L.; Baur, J. W., Effect of carbon nanotubes on the interfacial shear strength of T650 carbon fiber in an epoxy matrix. *Compos Sci Technol* **2009,** *69* (7-8), 898-904.

40. Stefanie Feih, K. W., Daniel Minzari, Peter Westermann, and Hans Lilholt *Testing procedure for the single fiber fragmentation test*; Risø National Laboratory: **2004**.

41. Yao, L. R.; Li, M.; Wu, Q.; Dai, Z. S.; Gu, Y. Z.; Li, Y. X.; Zhang, Z. G., Comparison of sizing effect of T700 grade carbon fiber on interfacial properties of fiber/BMI and fiber/epoxy. *Appl Surf Sci* **2012,** *263*, 326-333.

42. Weibull, W., A Statistical Distribution Function of Wide Applicability. *J Appl Mech-T Asme* **1951,** *18* (3), 293-297.

43. Toray Carbon Fibers America, I. Technical Data Sheet No. CFA-007. http://www.toraycfa.com/pdfs/T800HDataSheet.pdf.

44. Association, G. P., *Physical properties of glycerine and its solutions*. Glycerine Producers' Association: **1963**.

45. Boudaoud, A.; Burian, A.; Borowska-Wykret, D.; Uyttewaal, M.; Wrzalik, R.; Kwiatkowska, D.; Hamant, O., FibrilTool, an ImageJ plug-in to quantify fibrillar structures in raw microscopy images. *Nat Protoc* **2014,** *9* (2), 457-463.

46. Fu, S.-Y.; Lauke, B., Effects of fiber length and fiber orientation distributions on the tensile strength of short-fiber-reinforced polymers. *Compos Sci Technol* **1996,** *56* (10), 1179-1190.

47. Garoushi, S.; Lassila, L.; Vallittu, P., Short fiber reinforced composite: the effect of fiber length and volume fraction. *J Contemp Dent Pract* **2006,** *7* (5), 10-17.

48. Fu, Y. S.; Lauke, B., The elastic modulus of misaligned short-fiber-reinforced polymers. *Compos Sci Technol* **1998,** *58* (3), 389-400.

49. Jayaraman, K.; Kortschot, M. T., Correction to the Fukuda-Kawata Young's modulus theory and the Fukuda-Chou strength theory for short fibre-reinforced composite materials. . *J Mater Sci* **1996,** *31* (8), 2059-2064.

50. Piggott, M. R., Short fibre polymer composites: a fracture-based theory of fibre reinforcement. Journal of composite materials, . *J Compos Mater* **1994,** *28* (7), 588-606.

51. Fu, S. Y.; Lauke, B.; Mai, Y. W., Science and Engineering of Short Fibre Reinforced Polymer Composites. *Woodhead Publ Mater* **2009**, 1-338.

52. W, J. C. H. J. C. a. T. S. *Environmental factors in composite materials design* **1967**.